



Department of Aeronautical
and Automotive Engineering

Combustion Data Acquisition and Analysis

Benjamin Robert Brown (9633341)

Supervisor: Dr. Rui Chen

00TTD010: Final Year Project
M.Eng. Automotive Engineering

Summary

The acquisition and analysis of engine data provides an important insight into the complex phenomenon of combustion. In this report a comprehensive review of published literature is made and the development of an acquisition and analysis system is described. A new formula for the calculation of cylinder volume allowing for wrist pin offset is developed as well as techniques for solving particular problems associated with data acquisition. These include data acquisition triggered at the wrong TDC in an engine cycle, angular offsets between different cylinders and determining thermodynamic loss angle from motored engine pressure data. Finally, suggestions are made for future projects to add to and improve upon the work carried out.

Table of Contents

	List of Figures	
	Nomenclature	
1.0	Introduction	Page 1
2.0	Literature Review	Page 2
3.0	Data Acquisition	Page 16
4.0	Data Analysis	Page 28
5.0	Future Improvements	Page 49
6.0	Conclusions	Page 55
7.0	References	Page 56
Appendix A	Technical Specifications	Page 59
Appendix B	Equipment Calibration	Page 60
Appendix C	User Guides	Page 61
Appendix D	CD-ROM Contents	Page 67
Appendix E	Timing Plan	Page 68
Appendix F	Project Costs	Page 69

Acknowledgements

I would like to thank the technicians at the Aeronautical and Automotive Engineering department, notably Adrian Broster and Ted Smith for their invaluable help in setting up the acquisition hardware. Also, my supervisor Dr. Rui Chen for his constant enthusiasm and support for the project

List of Figures

- 3.1 Dynamometer speed calibration
- 3.2 Dynamometer torque calibration
- 3.3 Dynamometer throttle demand calibration
- 3.4 Fuel timer voltage output
- 3.5 Real time acquisition and analysis screenshot
- 3.6 Rover V8 throttle demand map
- 3.7 Rover V8 full load torque curves
- 4.1 Motored pressure data (Rover V8 – Motored – 3200RPM)
- 4.2 Thermodynamic loss angle (Rover V8 – Motored – 3200RPM)
- 4.3 Effects of firing order on acquired data (Rover V8 – Idle)
- 4.4 Corrected crank angle referencing (Rover V8 – Idle)
- 4.5 Calculated cylinder volumes verses crank angle for Rover V8 engine
- 4.6 Corrected pressure curves using polytropic process (Rover V8 – 3000RPM – WOT)
- 4.7 Calculated mass fraction burned curve (Rover V8 – 3000RPM – WOT)
- 4.8 Published values of the dynamic viscosity of air
- 4.9 Location of peak pressure (Rover V8 – 3000RPM – WOT)
- 4.10 pV Diagram, published figure⁸ (left) and analysis output (right)
- 4.11 Mean gas temperature, published figure⁸ (left) and analysis output (right)
- 4.12 Mass fraction burned, published figure⁸ (left) and analysis output (right)
- 4.13 Net heat release, published figure⁸ (left) and analysis output (right)
- 5.1 Recorded ignition voltage as indication of start of combustion⁸
- 5.2 Recorded fuel pressure as indication of start of combustion⁸
- 5.3 Recorded in-cylinder pressure and TDC marker data (Rover V8 – Engine Startup)
- B.1 Kistler 6125A calibration sheet (SN 573780)
- C.1 High speed data acquisition and analysis main panel
- C.2 Acquire Cylinder Data.vi main panel
- C.3 Running binary file conversion (fileweaver)
- C.4 Running combustion analysis (CAT)
- C.5 Excel text import wizard, step one
- C.6 Excel text import wizard, step two

Nomenclature

a	Annand heat transfer constant
A_s	Heat transfer surface area, Cubic metres
B	Cylinder bore, metres
C_m	Mean piston speed
C_p	Specific heat capacity at constant pressure
f	frequency
h	Heat transfer coefficient
kHz	kilo Hertz
L	Engine Stroke, metres
l	Conrod length
\dot{m}_{air}	Mass flow rate of air
\dot{m}_{fuel}	Mass flow rate of fuel
n	Polytropic index
N	Engine speed, RPM
N	Number of cycles
N_c	Engine speed, cycles per second
N_{max}	Maximum engine speed
p	Cylinder pressure
$p_{motored}$	Motored cylinder pressure
p_{ref}	Reference cylinder pressure
p_c	Pressure rise due to combustion
pC	pico Coulombs
p_v	Pressure rise due to volume change
p_c^*	Normalised pressure rise due to combustion
ΔP	Pressure transducer range
P_{brake}	Brake power
P_K	Peak knocking pressure
Q_{net}	Net heat release
Q_s	Instantaneous heat flow rate, Watts
R	Characteristic gas constant
Re	Reynolds number
R_{swirl}	Swirl ratio
r	Crank throw
s	Piston displacement
T	Mean gas temperature
T	Torque
T_{ref}	Reference mean gas temperature
T_{wall}	Wall temperature
V	Cylinder volume
V_{cr}	Crevice volume
V_{ref}	Reference cylinder volume
V_{swept}	Swept volume
W_i	Indicated Work
Z	Working fluid velocity

\bar{v}_p	Mean piston speed
λ	Gas thermal conductivity, kJ.m/s/K
μ	Dynamic fluid viscosity
σ	Stefan-Boltzmann constant
σ	Standard deviation
ν	Kinematic fluid viscosity
γ	Ratio of specific heats
θ	Crank angle
ρ_{air}	Density of air
ρ_{fuel}	Density of fuel
ϕ	Equivalence (Fuel Air) ratio
ω	Speed, radians/second

ADC	Analogue to Digital Converter
AFR	Air Fuel Ratio
AVL	AVL List GmbH
BDC	Bottom Dead Centre
BSFC	Brake Specific Fuel Consumption
BTDC	Before Top Dead Centre
BMEP	Brake Mean Effective Pressure
CI	Compression Ignition
COV	Coefficient Of Variance
CR	Compression Ratio
DSP	Digital Signal Processing
ECU	Electronic Control Unit
EEOC	Estimated End Of Combustion
EGR	Exhaust Gas Recirculation
FEAD	Front End Accessory Drive
FFT	Fast Fourier Transform
IDI	Indirect Injection
IMEP	Indicated Mean Effective Pressure
KI	Knock Intensity
LCV	Lower Calorific Value
LNV	Least Normalised Value
MFB	Mass Fraction Burned
PC	Personal Computer
PLL	Phase Locked Loop
RPM	Revolutions Per Minute
RTV	Room Temperature Vulcanising
SI	Spark Ignition
TDC	Top Dead Centre
TLA	Thermodynamic Loss Angle
WOT	Wide Open Throttle

1.0 Introduction

The recording and analysis of engine data has long been used in both industry and academia as a way of quantifying engine-operating characteristics. The most useful quantity to record is in-cylinder pressure, as the analysis of the pressure and parameters derived from the pressure can tell us a great deal about the complex process of combustion.

Various methods of recording engine data are possible. In conventional applications data is recorded with a fixed acquisition rate, whereby the time interval between two subsequent recordings is fixed.

However, because an engine runs in a cycle dictated by a set of mechanical mechanisms – slider-crank, poppet valves, etc – and because these mechanisms have fundamental consequences to how combustion takes place, it is necessary to record data at known crank angle intervals.

The aim of this project is to provide a documented process to acquire and process engine data referenced to crank angle. Once data has been accurately recorded it can be further analysed to provide key indicators of engine performance.

Combustion analysis is used both in industry and academia as a convenient method of quantifying the effects of modifications to engine design and calibration and their effect on speed and completeness of combustion.

The project will have various uses:

Engine development – in the calibration of engine control systems and the design of engine components.

Engine testing – in combination with a programmable ECU the system could control an engine and record combustion data, i.e. spark timing sweeps measuring IMEP.

Engine control – to research closed-loop control strategies using cylinder pressure or knock control.

Teaching tool – to support thermodynamic and IC engine courses to demonstrate cylinder pressure data acquisition and the derived parameters.

This project has been initiated because the Aeronautical and Automotive Engineering department at Loughborough University has no current and documented system for carrying out such data acquisition and analysis. The completed system would allow data to be both acquired and analysed quickly to allow quick turnaround of combustion comparisons.

This report begins with a literature review, where a substantial amount of published work has been condensed to cover key areas of acquisition and analysis technology. Because the project consists of two different technology areas – data acquisition and data analysis these have been separated into two sections. Finally, as the project aims to build a firm basis for further work, a section is dedicated to improvements to the implemented system and how it can be expanded in the future.

2.0 Literature Review

This literature review has broken down the key areas of a combustion analysis system into acquisition hardware, signal processing, data validation and parameter calculation.

2.1 Hardware

The requirements of a combustion data acquisition system are to record cylinder pressure data and align it to cylinder volume data. This is achieved by using a triggered acquisition, (acquisition does not begin until TDC is reached), and sampling using an external clock, (one acquisition per clock pulse). In addition to cylinder pressure data other parameters may be measured including:

- Inlet or exhaust manifold pressure
- Spark current
- Injector needle lift
- Fuel pressure
- Engine angular velocity
- Acceleration of engine components

2.1.1 ADC Resolution

The analogue to digital converter (ADC) resolution determines the minimum amount of pressure change that can be recorded. The actual minimum value of pressure is given by:

$$\Delta p = \frac{\Delta P}{2^r} \quad \text{(Equation 2.1)}$$

where ΔP is the total pressure range (typically 100 bar) and r is the bit resolution of the ADC. Minimum resolutions for typical pressure ranges are given in Table 2.1.

Resolution (bits)	50 bar range	100 bar range	250 bar range
8	195.32	390.63	976.58
10	48.83	97.66	244.15
12	12.21	24.41	61.03
14	3.05	6.10	15.25
16	0.77	1.53	3.83

Table 2.1 – Minimum pressure measurement of ADCs in Pascals

Clearly a lower range and greater ADC resolution will provide a more sensitive acquisition, and as explained by Brunt et al²⁰ can help to reduce noise levels in derived parameters. However, high-resolution ADC converters are more expensive and limiting the pressure transducer range is inappropriate for many applications.

Brunt et al³ used an AVL 670 Indimaster which was fitted with 14-bit analogue to digital converter cards.

Kim et al¹² used an ADC with 12 bit resolution with 15 microsecond conversion rate.

2.1.2 Triggering

In order to phase the measured data with the cylinder volume it is necessary to accurately determine at what point in the engine's thermodynamic cycle the data acquisition started. A common method is to begin the acquisition when the crank is at TDC.

This has the disadvantage that the recorded data may begin at either compression TDC or exhaust TDC. A simple check can be used to correct this by comparing data acquired at zero and 360 degrees. The pressure will be greater at compression TDC than exhaust. Hence if the pressure at zero degrees is greater than at 360 degrees, the first 360 degrees of pressure data should be discarded. If a specific number of cycles is to be acquired then an extra 360 degrees should be acquired for this purpose and discarded if no correction is required.

2.1.3 External Clock

Engine rotational velocity will always vary with time due to cycle-to-cycle variability in combustion timing and strength. It is therefore not possible to acquire data with a clock frequency dependent on engine speed and still accurately align measured data with the corresponding cylinder volume. Hence an external clock is used. This provides a Phase Locked Loop (PLL) signal that indicates when a certain amount of engine rotation has occurred.

Kim et al¹² used a aluminium disk and photo sensor to give 1440 pulses per revolution (0.25 degree intervals).

Lancaster et al¹¹ used a photo-electric pulse generator giving 360 pulses per revolution (1 degree intervals).

2.1.4 Pressure Transducers

Piezoelectric pressure transducers are the most commonly used form of pressure transducer for the purpose of acquiring in-cylinder pressure data. They however have several disadvantages, these include sensitivity to thermal shock, long and short-term drift, sensitivity to temperature and that the output has to be referenced to an absolute pressure. Transducer drift increases the measured cyclic variability.

2.1.5 Charge Amplifiers

Lancaster et al¹¹ notes that charge amplifier range and time constants should be set to give the longest system time with minimal signal drift. The time constant of a piezoelectric system is a measure of the time for a given signal to decay, not the time it takes the system to respond to an input.

It is important that all connections between the charge amplifier and transducer be degreased with contact cleaner. This is because low insulation resistance in the transducer or cables and connection causes drift of the charge amplifier output. Lancaster et al¹¹ suggests that the charge amplifier is allowed to warm up for one hour before measurements are taken.

2.1.6 TDC Determination

Lancaster et al¹¹ notes that since physical dimensions of the engine can be determined quite accurately, the accuracy of the total volume calculation is limited by the accuracy of both the clearance volume measurement and the determination of crank angle.

TDC must be determined within 0.1 degrees in order to accurately calculate work (IMEP) and can generally be determined using a dial-gauge during engine construction or by determination of the line of symmetry of motored engine pressure data.

Dynamic TDC, i.e. the actual TDC taking into account piston stretch and crankshaft twist, is described by Kim et al¹² by the use of microwave and proximity probes. The use of more accurate methods of dynamic TDC determination show that in order to avoid serious error in the TDC determination caused by torsional vibration the test cylinder must be chosen in a multi-cylinder engine as the one immediately next to the crankshaft encoder.

2.2 Signal Processing

2.2.1 Analogue Filtering

Brunt et al³ notes the use of AVL charge amplifiers fitted with 120 kHz analogue filters.

2.2.2 Digital Filtering

Brunt et al³ use a 20 kHz low pass digital filter (second order Butterworth) to remove effect of Kistler 6125A transducer natural frequency for knock analysis.

2.2.3 Pressure Pegging

As piezoelectric pressure transducers produce a charge relative to change in pressure levels, therefore a method is therefore required to peg recorded pressure data to absolute levels. Randolph¹⁰ describes a number of methods for pegging absolute cylinder pressures. The two main types of pegging described are setting a point within the engine cycle to a known or estimated pressure and fitting the compression to a polytropic process.

Randolf³⁴ notes that determination of IMEP, variability in IMEP, PMEP, maximum rate of pressure rise and location of peak pressure do not require pegged data. It is only absolute metrics such as peak pressure that require pegged data.

Randolf¹⁰ notes that short-term pegging (i.e. every cycle) removes the problems of long-term drift inherent in piezoelectric devices and those techniques that use mechanical switching as an indicator for absolute pressures are too slow for cycle-resolved use.

Brunt¹ notes that higher absolute accuracy is generally needed for combustion analysis at low load and under slow burn conditions and that high accuracy is only achievable with the absence of all other sources of error throughout the whole cycle. Thermal shock, long term drift and sensitivity errors mean accurate pressure referencing will occur over a limited portion of the engine cycle.

Randolf¹⁰ notes that intracycle drift, the drift that occurs between the beginning and end of a single cycle, is of greater importance than long-term drift. He identifies that intracycle drift can be measured by the difference in transducer output at IBDC (before pegging) for any two consecutive cycles.

Brunt¹ therefore concludes that it is necessary to decide which part of the cycle needs accurate referencing. Accurate referencing of induction and exhaust pressures for example will be of critical importance for breathing and friction studies but will be of much less importance for combustion analysis.

Reference Pressure

Randolf¹⁰ found that for the engine used in his study referencing the transducer output at inlet bottom dead centre (IBDC) to intake manifold pressure (MAP) performed best. However, this is only true for engines with untuned intake systems or at very low speeds in tuned systems. He notes that any type of runner will generate tuning effects, thereby limiting this method to low engine speeds. To reduce the effects of noise the inlet manifold

pressure was the average of the transducer output at one degree before IBDC, at IBDC and one degree after IBDC.

Lancaster et al¹¹ says: Cylinder pressure data is pegged by assuming the pressure at BDC after the intake stroke is equal to the mean intake manifold pressure.

Through experience Hayes et al¹⁷ set the cylinder pressure 40 degrees before IBDC equal to the manifold pressure.

Polytropic

Pressure correction is applied to each point of cycle data by:

$$P_{actual} = P_{measured} + P_{correction} \quad (\text{Equation 2.2})$$

where

$$P_{correction} = \frac{P_2 - P_1}{\left(\frac{V_1}{V_2}\right)^n - 1} - P_1 \quad (\text{Equation 2.3})$$

where P_n and V_n are the pressures and volumes respectively of data in the compression region.

Randolf¹⁰ used a constant polytropic coefficient, n , of 1.32, and quotes Hohenberg and Killmann as using 1.32 for homogeneous-charge engines and 1.27 for Diesel engines).

Randolf¹⁰ suggests that to minimize variability from slope computation (of polytropic coefficient) it is advisable to maximise the number of measurements and the crank angle spread of those measurements when calculating the polytropic compression coefficient. However, it must remain between intake-valve closure and ignition.

Brunt et al¹ quotes AVL as suggesting a polytropic index of 1.32 between 100 and 65 degrees BTDC, whilst Kistler's 5219A signal conditioner uses 1.35 between 120 and 70 degrees BTDC. Brunt et al¹ also notes that the polytropic method is more sensitive to noise spikes than pressure referencing, but this can be reduced by increasing the upper crank angle. Their conclusions are that polytropic indexing is the best method for pegging, however it is unsuitable for situations where a polytropic index is unknown, such as weak mixtures.

2.2.4 Thermal Shock

Thermal shock is a major problem with piezoelectric pressure transducers when trying to make accurate cylinder pressure measurements.

From Brunt et al⁴:

- Cyclic exposure of a piezoelectric pressure transducer to combustion results in the expansion and contraction of its diaphragm due to large temperature variations

throughout the cycle. This causes the force on the quartz to be different to that applied by the cylinder pressure alone.

- Thermal shock affects all parameters derived from pressure data, but the greatest is IMEP, which can be affected by over 10%.
- Thermal shock was found to be most significant at low engine speeds, high loads, advanced ignition timings, slightly rich mixtures and low EGR.
- Equation developed to compensate for thermal shock of a Kistler 6125A transducer:

$$IMEP_{corr} = IMEP_{meas} + (FxP_{max}) + Offset \quad (\text{Equation 2.4})$$

where:

$$F = 0.000133 \left(\frac{rpm}{1000} \right)^2 - 0.002 \left(\frac{rpm}{1000} \right) + 0.0105 \quad (\text{Equation 2.5})$$

$$Offset = 0.012 \left(\frac{rpm}{1000} \right)$$

- Transducer location did not have a significant effect on thermal shock.
- RTV coating was found to be effective in reducing thermal shock.
- IMEP errors for the Kistler 6125A were reduced from a maximum of -4.9% to between -0.4% and $+0.8\%$.
- Equation 2.5 has been developed for the Ford Zetec engine; further work is required to determine performance of algorithm with other engine designs.

2.3 Data Validation

From Lancaster et al¹¹:

- In terms of screening acquired data, Brown is quoted, “consistency is no indication of accuracy.”
- Motored pressure data exhibits little cycle-to-cycle variability and can therefore yield significant information about the accuracy and reliability of the test set-up and recording procedure.
- Peak pressure in a motored engine occurs before TDC due to irreversibility caused primarily by heat transfer and the additional lag from measuring pressures in an IDI CI engine. Kim et al¹² calls this the thermodynamic loss angle (TLA) and is calculated as the crank angle difference between the dynamic TDC and the motored peak pressure angle.
- Kim et al¹² find the peak pressure angle using a best fit curve of cylinder pressure data within 20 degrees before and after the peak. They note that heat loss per engine cycle and mass blow by loss will reduce with increasing engine speed. This results in the motoring peak pressure shifting towards TDC with increased speed.
- During intake, at the part of the engine cycle where the instantaneous gas flow rate is high, the cylinder pressure should fall below the measured mean intake manifold pressure.
- The fact that motored engine IMEP is non-zero is one source of estimating the error in IMEP for a fired engine.
- An excellent test of motoring pressure data is a direct comparison to computer simulation data.
- Brown is quoted as indicating that a crank angle phase error of less than 0.1 degrees is required for accurate (less than 1% error) IMEP calculations for a CI engine. This can be relaxed to 0.2 to 0.3 degrees for SI engines.

2.4 Parameter Calculations

From Lancaster et al¹¹:

- One of the most useful quantities obtainable from cylinder pressure measurements is engine friction.
- Engine pumping losses are an important aspect of engine performance, especially at part load.
- Pressure data can also be used to compare against computed engine simulation
- The engine itself is an averaging device that responds to mean values of air and fuel flows by generating a mean indicated power. Therefore, it is appropriate to use the mean of many cycles to calculate quantities.

Randolph³⁴ notes that cylinder pressure measurements can provide information regarding cylinder balance, cyclic torque variability, combustion phasing, detonation, structural loading, intake and exhaust tuning, thermal efficiency and cyclic fuelling variability.

2.4.1 Volume Determination

From Lancaster et al¹¹:

- Accuracy of volume calculation is limited by the clearance volume measurement (compression ratio) and the determination of the crank angle.
- Clearance volume is not required for the determination of mean effective pressure.

2.4.2 Gamma

From Brunt et al⁶:

- Gamma (γ) is the ratio of specific heats. A low value of gamma produces heat release value that is too high and a heat release rate that is negative after the completion of combustion.
- A temperature dependent equation for gamma is produced from experimental data:

$$\gamma = 1.338 - 60 \times 10^{-5} \cdot T + 1.0 \times 10^{-8} \cdot T^2 \quad (\text{Equation 2.6})$$

- Gamma is also dependent on equivalence ratio, ϕ . The effect of ignoring this term is an error of up to ± 0.015 in gamma ($0.8 < \phi < 1.2$)

Hayes et al¹⁷ and Rocco¹⁸ present Zucrow and Hoffman's equations of gamma:

$$\gamma = \frac{\bar{C}_p}{\bar{C}_p - R} \quad (\text{Equation 2.7})$$

for $T < 1000\text{K}$

$$\bar{C}_p = \left(3.6359 - \frac{1.33736T}{1000} + \frac{3.29421T^2}{1 \times 10^6} - \frac{1.91142T^3}{1 \times 10^9} + \frac{0.275462T^4}{1 \times 10^{12}} \right) \bar{R}$$

(Equation 2.8)

for $T > 1000\text{K}$

$$\bar{C}_p = \left(3.04473 + \frac{1.33805T}{1000} - \frac{0.488256T^2}{1 \times 10^6} + \frac{0.0855475T^3}{1 \times 10^9} - \frac{0.005701327T^4}{1 \times 10^{12}} \right) \bar{R}$$

(Equation 2.9)

The main advantage of temperature dependent gamma is that it adjusts to different engine operating conditions – higher values of gamma would be used at low engine load.

2.4.3 Pressure

Parameters of interest include magnitude and crank angle of maximum pressure and magnitude and crank angle of maximum pressure rise rate. Brunt¹⁶ quotes Ricardo, that for maximum efficiency pressure rise rate should be 2.3 bar/degree and that Janeway has shown the gradient of pressure rise rate should be kept to a minimum for smooth operation.

2.4.4 Indicated Mean Effective Pressure (IMEP)

The area enclosed by the p-v diagram of an engine is the indicated work done by the gas on the piston. The imep is a measure of the indicated work output per unit swept volume, a parameter independent of the size and number of cylinders in the engine and engine speed.

IMEP is defined as⁸:

$$imep = \frac{W_i}{V_s}$$

(Equation 2.10)

where

W_i is the indicated work in Newton metres

V_s is the swept volume per cylinder in cubic metres

Brunt¹ notes that imep is highly sensitive to crank angle phasing errors and thermal shock, virtually insensitive to random noise and totally unaffected by absolute pressure referencing errors.

From Brunt¹⁴ et al:

- Errors in calculated IMEP are mainly caused by thermal shock, crank angle phasing errors and transducer sensitivity,
- Coarse crank angle resolution, incorrect con rod length, signal noise and integration period error should produce relatively small errors.
- An IMEP formula is identified which is resilient to large crank angle resolution:

$$imep = \frac{\Delta\theta}{V_s} \sum_{i=n_1}^{n_2} p(i) \cdot \frac{dV(i)}{d\theta} \quad (\text{Equation 2.11})$$

where

$p(i)$ is cylinder pressure at crank angle i in Pascals
 $V(i)$ is cylinder volume at crank angle i in cubic metres
 V_s is cylinder swept volume in cubic metres
 n_1 is BDC induction crank angle
 n_2 is BDC exhaust crank angle

The coefficient of variance (CoV) in IMEP has proven useful in evaluating combustion-chamber designs and is given by¹⁹:

$$C_v = \frac{\sqrt{\frac{\sum (p_i - \bar{p}_i)^2}{(N-1)}}}{\bar{p}_i} \quad (\text{Equation 2.12})$$

where

N is the number of cycles sampled.

2.4.5 Burn Rate

From Rassweiler and Withrow¹³:

- Throughout the entire combustion period the value of the per cent mass fraction burned at any given crank angle is very nearly equal to the per cent pressure rise due to combustion at that same angle.

From Brunt et al²

- Rassweiler and Withrow method for burn rate analysis is both accurate and computationally efficient.
- Largest errors occur when:
 - absolute pressure errors exist in low load conditions due to the incorrect polytropic index calculation
 - pressure data errors exist when calculating <10% and >90% burn angles
 - less than 100 cycles are recorded
 - slow burns, partial burns and misfires are present
- Accurate calculation of 5% and 95% burn angles are difficult without good pressure data.
- Burn angles calculated from average cycle data is acceptable except when large cyclic variations are present.
- A minimum of 150 cycles at 1 degree resolution should be adequate for burn rate analysis.

- An estimated end of combustion (EEOC) algorithm is described that determines the normalising factor for cumulative MFB curves and calculation of expansion curve immediately following combustion.

From Stone⁸:

- Wiebe function describes mass fraction burned profile using two constants, a and m. Typically, a=5 and m=2. Wiebe function is of the form:

$$x(\theta) = 1 - e^{-a \left(\frac{\theta - \theta_0}{\Delta\theta_b} \right)^{m+1}} \quad (\text{Equation 2.13})$$

where

$x(\theta)$ is the mass fraction burned at crank angle θ

θ_0 is the crank angle at the start of combustion

$\Delta\theta_b$ is the duration of combustion

To support engine-modelling programs the analysis software should be capable of determining the Wiebe function.

From Cheung et al¹⁵:

- Equations are proposed for a burn-rate model that includes models for crevice flows and residual gas mass fractions.
- Mass fraction curves are calculated that do not reach 100% and show misfiring cycles.
- Extra data required include R_{swirl} , the swirl ratio, V_{cr} the crevice volume, inlet and exhaust pressures, valve overlap and fuel-air equivalence ratio.
- Wall temperature for heat transfer calculations is determined by equivalence ratio:

$$T_{wall} = 400\text{K for } \phi < 0.833$$

$$T_{wall} = 425\text{K for } 0.833 < \phi < 0.9$$

$$T_{wall} = 450\text{K for } 0.9 < \phi$$

Proposed model is shown to be reasonable for low speed cases, but not for medium and high speeds.

2.4.6 Heat Release

From Brunt et al⁶:

- Burn rate analysis is mainly used to determine burn angles in gasoline engines.
- Heat release analysis is most commonly used in Diesel engines and produces absolute energy figures with units Joules or Joules/degree.
- Accuracy required depends on application. Laboratory experiments require high accuracy, but for routine engine development consistency and repeatability rather than accuracy are more important.

- Net heat release figures are typically 15% lower than gross figures.
- Heat transfer can be modelled using the Annand heat transfer equation.

From Ganesan⁷ and Stone⁸:

Different correlations of in-cylinder heat transfer are used to determine net figures of heat release. The correlations are given in the form:

$$h = \frac{Q_s}{A_s(T - T_s)} \quad \text{(Equation 2.14)}$$

where Q_s is the instantaneous heat flow rate in Watts, A_s is the instantaneous heat transfer surface area, T is the working fluid temperature in Kelvin and T_w the interior surface temperature in Kelvin.

- Ashley-Campbell

$$h_c = 0.13B^{0.12} p^{0.8} T^{-0.5} Z^{0.8} \quad \text{(Equation 2.15)}$$

- Nusselt

$$h_c = 0.99(1 + 1.24C_m)(p^2 T)^{2/3} \quad \text{(Equation 2.16)}$$

- Briling

$$h_c = 0.99 + (3.5 + 0.185C_m)(p^2 T)^{2/3} \quad \text{(Equation 2.17)}$$

- Eichelberg

$$h_c = 2.1C_m^{2/3} (pT)^{1/2} \quad \text{(Ganesan)} \quad \text{(Equation 2.18)}$$

$$h = 2.43C_m^{1/3} (p.T)^{1/2} \quad \text{(Stone)} \quad \text{(Equation 2.19)}$$

- Annand

$$h_c = a \left(\frac{\lambda}{B} \right) \text{Re}^{0.7} + \frac{C}{T - T_w} x \left[\left(\frac{T}{100} \right)^4 - \left(\frac{T_w}{100} \right)^4 \right] \quad \text{(Ganesan)} \quad \text{(Equation 2.20)}$$

$$h = a \left(\frac{\lambda}{B} \right) \text{Re}^{0.7} + \frac{C}{(T - T_w)} (T^4 - T_w^4) \quad \text{(Stone)} \quad \text{(Equation 2.21)}$$

where

B is cylinder bore in metres

p is cylinder pressure in bar

T is working fluid temperature in Kelvin

T_w is interior surface temperature in Kelvin

Z is working fluid velocity in metres per second

C_m is mean piston speed in metres per second

Stone suggests:

$$0.25 < a < 0.8$$

$C = 0.576\sigma$ for a CI engine
 $C = 0$ for a CI engine during intake compression and exhaust processes
 $C = 0.075\sigma$ for a SI engine
 σ is the Stefan-Boltzmann constant

Ganesan suggests:

a equals 0.35 to 0.8 increasing with increasing engine speed
 C equals 0 for compression stroke of SI engine, 0.37 for other strokes and 2.81 for CI engines
 λ is gas thermal conductivity in $\text{kJ/s}\cdot\text{m/K}$
 Re is Reynolds number

- Woschni

$$h = 129.8 p^{0.8} u^{0.8} B^{-0.2} T^{-0.55} \quad (\text{Equation 2.22})$$

where

$$u = C_1 \bar{v}_p + C_2 \frac{V_s T_r}{p_r V_r} (p - p_m) \quad (\text{Equation 2.23})$$

V_s is swept volume

V_r , T_r and p_r are evaluated at any reference condition, such as inlet valve closure.

Values suggested for C_1 and C_2 by Annand:

For gas exchange:	$C_1 = 6.18$	$C_2 = 0$
For compression	$C_1 = 2.28$	$C_2 = 0$
For combustion and expansion	$C_1 = 2.28$	$C_2 = 3.24 \times 10^{-3}$
For IDI engines		$C_2 = 6.22 \times 10^{-3}$

Hayes et al¹⁷ used the Eichelberg correlation. The combustion chamber was assumed to be 450°C and the surface area was calculated assuming a cylindrical disc.

2.4.7 Knock Intensity

From Checkel & Dale⁵:

- An algorithm is developed to indicate knock from pressure records.
- Knock is quantified by the peak negative value of third differential of pressure over the crank angle where knock is expected.
- Method is successfully used with acquisition rate of one-degree resolution.
- Basic differentiator equation is:

$$dp(\theta) = \frac{(86.(p_{\theta-4} - p_{\theta+4}) + 142.(p_{\theta+3} - p_{\theta-3}) + 193.(p_{\theta+2} - p_{\theta-2}) + 126.(p_{\theta+1} - p_{\theta-1}))}{1188.d\theta} \quad (\text{Equation 2.24})$$

- Digital low-pass filter (applied between second and third differentiations):

$$F(\theta) = \frac{(2.(S_{\theta-4} + S_{\theta+4}) + 3.(S_{\theta-3} + S_{\theta+3}) + 4.(S_{\theta-2} + S_{\theta+2}) + 5.(S_{\theta-1} + S_{\theta} + S_{\theta+1}))}{33}$$

(Equation 2.25)

From Brunt et al³

- At least 1000 engine cycles is recommended for knock intensity determination.
- A knock window of TDC to TDC+40 degrees has been shown to be appropriate.
- 0.2 degree crank angle resolution considered to be adequate for the knock algorithm employed. Knock intensity is reduced with coarser crank angle resolution.
- AVL 670 Indimaster carried out signal acquisition and processing using 14-bit analogue to digital converter cards. AVL charge amplifiers fitted with 120 kHz analogue filters. Flywheel trigger pulses at 0.05 degree resolution.
- Non-flush mounting of pressure transducers can cause problems with cavity resonance.
- Centrally mounted pressure transducers (such as spark plug transducers in four valve engines) can be insensitive to circumferential modes, but still detects the weaker radial modes.
- Sampling rate of circa 300 kHz is required to ensure unwanted high frequency signals are not present.
- Kistler 6125A transducer is identified as having its natural frequency around 70 kHz. A 20 kHz low pass digital filter (second order Butterworth) was applied to all pressure data to remove the effect of the transducer natural frequency.
- Knock vibrational modes are typically in the range 6 to 20 kHz for automotive sized engines.
- Primary metric of knock level was the peak knock pressure. This was defined as the maximum positive value of the high frequency pressure component.
- A moving average of nominally ± 2 degrees was applied to the pressure data. This was altered as a function of engine speed on the basis of a primary knock mode frequency of 7.0 kHz.
- Non-knocking peak knock pressures were of the order 0.2 bar.
- Knock intensity was calculated as:

$$KI = \frac{20}{N_c} \sum (P_k - 1.0)$$

(Equation 2.26)

where

N_c is the number of cycles and P_k is the peak knock pressure.

- Validation of this method was made against a FFT spectral analysis knock model and the Checkel & Dale third derivative knock model.

3.0 Data Acquisition

3.1 Introduction

The initial focus of the project was to determine what, if any, suitable hardware and software was available in the department. From the literature review carried out it was identified that the following components would be required:

- Dynamometer and engine
- Pressure transducer
- Charge amplifier
- TDC marker
- Crank angle encoder
- PC with data acquisition hardware of suitable acquisition rate

3.2 Hardware Setup

A Rover V8 engine was available which was already fitted with suitable tapings in the cylinder head to take Kistler pressure transducers. A Kistler 6125A piezoelectric pressure transducer and a Kistler 5011 charge amplifier were also available to the project. The calibration sheet for the Kistler transducer was located giving the transducers sensitivity as -15.8 pC/bar at a 0-250 bar operating range. However, as can be noted from the calibration sheet, figure B.1, the calibration date was November 1995, some five years previous.

Unfortunately, before the completion of testing the Kistler 6125A pressure transducer became loose and dropped into the combustion chamber whilst the engine was running. This caused permanent damage to the transducer. However, some searching located two Kistler 6121 pressure transducers. Although having a slightly lower technical specification to the 6125A transducers they fit in the same cylinder head tapings, and by obtaining a second Kistler 5011 charge amplifier, two in-cylinder pressures could be acquired simultaneously. Unfortunately, the two sensors were without calibration sheets and hence a nominal sensitivity of -15.5 pC/bar was used to calibrate the charge amplifier. Although this leads to incorrect pressure data, it was decided that the scope of the project was to develop a system capable of acquiring valid engine data and this would be so with the correct calibration available.

The Kistler 5011 charge amplifiers were set with medium time constant and the inbuilt analogue filter was turned off.

A number of absolute pressure transducers were located on other engine dynamometers in the department and an adapter was made to fit one to the Rover's inlet manifold. The absolute pressure of the inlet manifold could be used to investigate the different methods of absolute pressure correction of the piezoelectric pressure transducers.

The literature review had highlighted the importance of accurate crank angle measurements, particularly the determination of TDC. Therefore some time was spent on determining the best method of crank angle measurement available.

The engine was already fitted with a hall effect sensor mounted on the gearbox bellhousing that would sense the flywheel ring gear. This was amplified and processed to produce a phase locked loop (PLL) signal with one-degree crank angle resolution. Another hall effect sensor was located on a bracket attached to the bellhousing that produced a pulse each time a small pin on the flywheel passed it, hence locating TDC.

The possibility of fitting a more accurate crank encoder was investigated, however it was decided to use the existing hall effect sensors for a number of reasons. Firstly the encoders in possession by the department consisted of finely marked glass discs, which although encased, were easily broken. This was especially true when connected to the vibrations of an engine, whereas the hall effect sensors were much more robust. Secondly, fitment of the encoder would require the strip down of the engine's front end accessory drive (FEAD) and the design and manufacture of a suitable bracket and drive. Although this would have been within the scope of the project to implement, it was decided not to pursue this in order to progress the project in a timely fashion.

The department had recently purchased a PC and National Instruments data acquisition card with a high data acquisition rate (200 kHz). In order to determine if this rate was suitably high a formula, equation 3.1, was developed.

$$f = \frac{N_{max}}{60} \times R \times C \quad (\text{Equation 3.1})$$

where

- f is the required acquisition frequency in Hz
- N_{max} is the maximum engine speed in RPM
- R is the acquisition resolution (pulses per revolution)
- C is the number of channels of data to acquire

Using this formula, for a 200 kHz maximum acquisition rate, one-degree crank angle resolution (360 pulses per revolution) and a maximum engine speed of 6500RPM, up to five channels of data can be recorded.

The dynamometer provided eight coax cable lines between break out boxes located next to the engine and on the dynamometer control panel. This provided an easy means of connecting the various sensor signals to the acquisition PC. In order to minimise the effects of noise and signal leakage all connectors were cleaned with greaseless contact cleaner and connections were disconnected and reconnected prior to usage to ensure good electrical contact. Where possible cables were routed away from power cables and high temperature surfaces using the minimum amount of cable length and connectors.

3.3 Raw Signal Validation and Calibration

3.3.1 Crank Angle Signal

At an idle speed of 830RPM (according to the dynamometer controller) the oscilloscope showed a PLL pulse from the crank position sensor approximately every 200 μ s, which equates to an engine speed of 830RPM.

3.3.2 TDC Marker

At the same 830RPM idle speed a TDC pulse was occurring every 72ms that equates again to an engine speed of 830RPM. The positioning of the pin to relate to TDC of cylinder one was carried out using a method described by Lancaster et al¹¹.

The position of cylinder one TDC was initially estimated using a dial gauge placed through the spark plug hole. This is only an estimate because firstly the spark plug whole location does not allow the dial gauge to be place perpendicularly to the piston crown and secondly the movement of the piston at TDC is very small, making the exact point of TDC difficult to establish.

A more accurate determination of TDC was made using a large change of piston position either side of TDC by 30 degrees and then marking the flywheel at both positions. The marks were then bisected to give TDC position. With no wrist pin offset this provides an accurate determination, however most engines include an offset to reduce the effects of piston slap. However, Lancaster shows the error introduced to be less than 0.06 of a degree.

3.3.3 Charge Amplifier Output

For an 830RPM idle speed a continuously updated acquisition was carried out with 4980 Hz sampling rate, calculated using equation 3.1, and 720-point (degree) output graph. Allowing for the unstable idle speed this showed one entire engine cycle was successfully being acquired from the charge amplifier.

3.3.4 Inlet Manifold Pressure

The pressure transducer fitted to the inlet manifold is a TransInstruments absolute pressure transducer with 0-1.6 bar range and 0-5v output. As no calibration was available for this instrument a linear correlation of 0.32 v/bar was assumed. This provided a 1.0 bar output at atmospheric conditions.

3.3.5 Dynamometer Outputs

The output signals of the dynamometer were calibrated by plotting the analogue voltage output measured by the data acquisition card and the values output on the dynamometer control panel. Due to the noise and changing values this was done over a wide range of values and on different days to ensure wide scale accuracy. Data was plotted and a line of best fit calculated. Plots of dynamometer speed, torque and throttle demand are shown in figures 3.1 through 3.3, as well as equations for the lines of best fit.

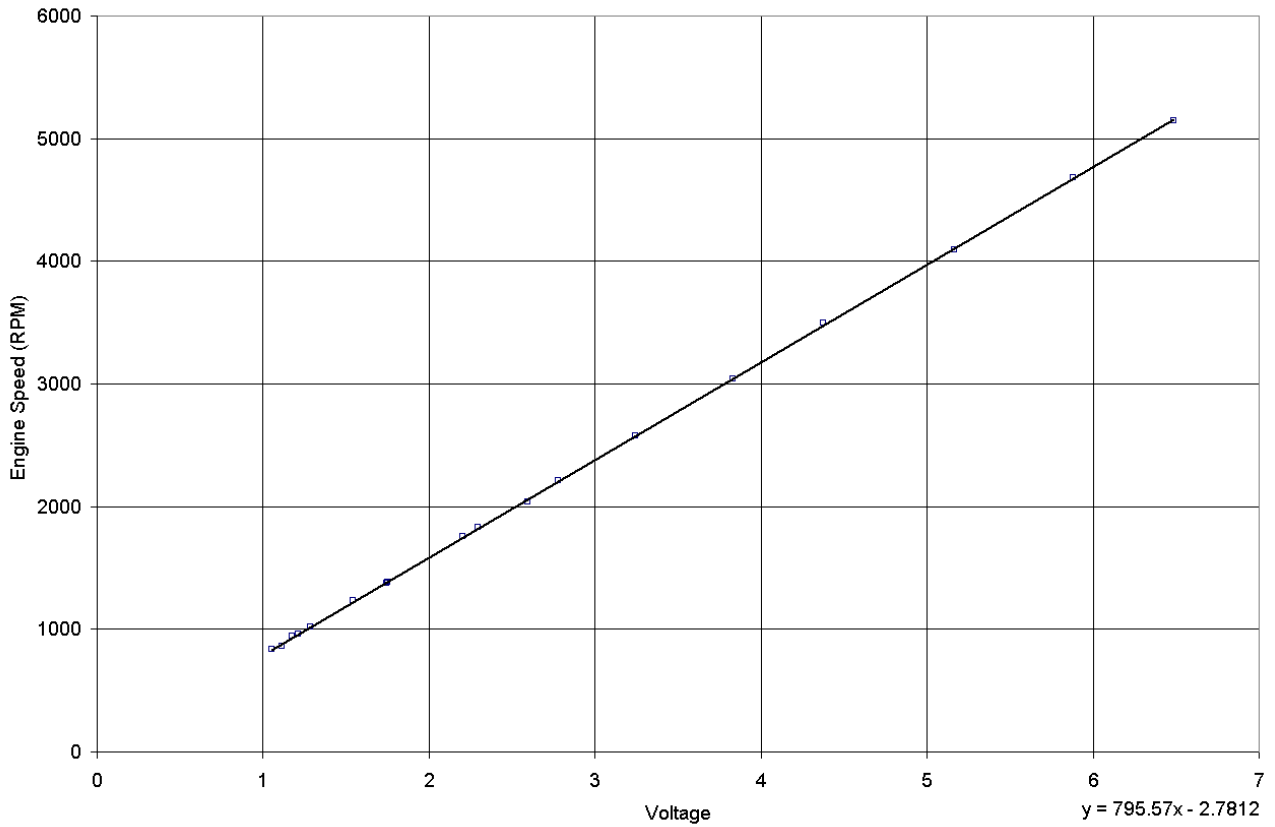


Figure 3.1 – Dynamometer speed calibration

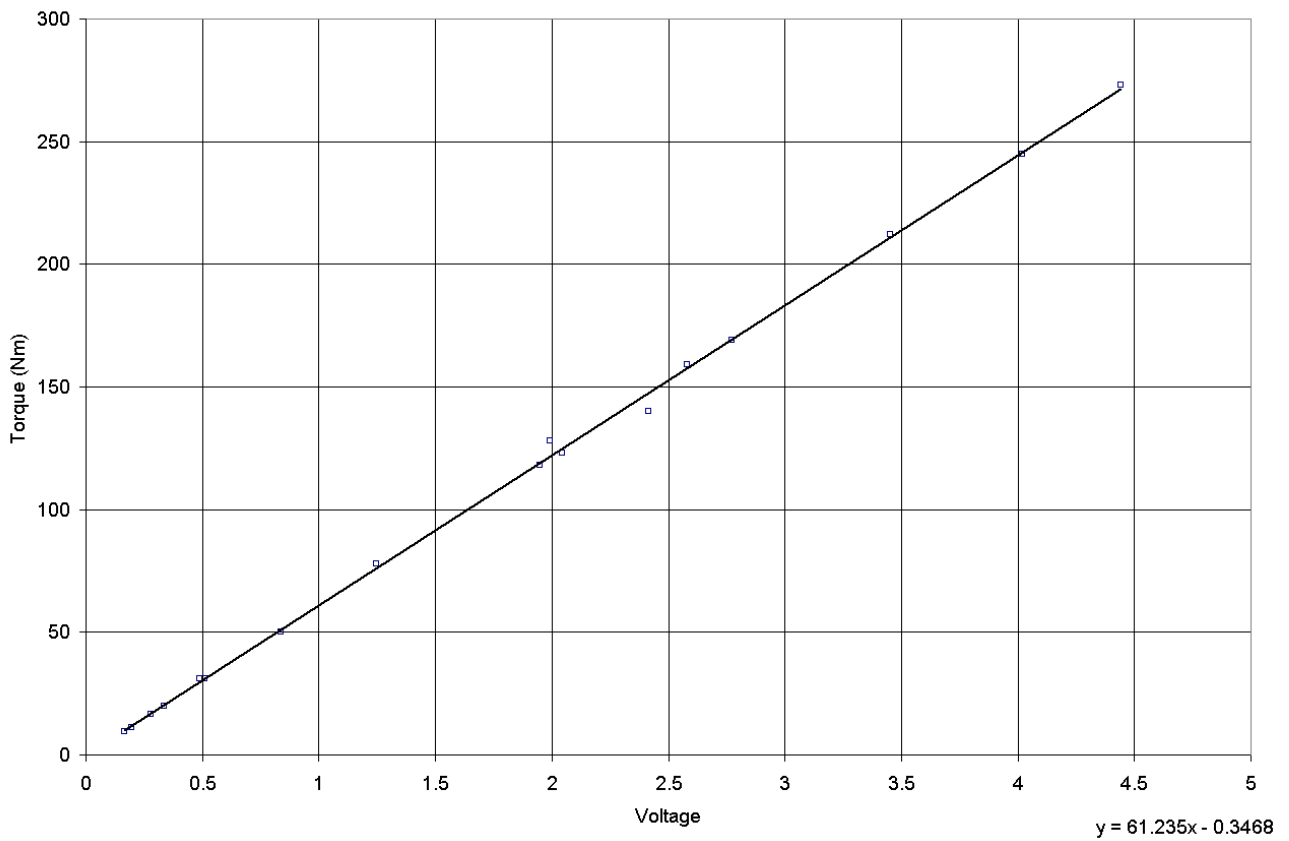


Figure 3.2 – Dynamometer torque calibration



Figure 3.3 – Dynamometer throttle demand calibration

3.3.6 Fuel Timer

The fuel timer fitted to the dynamometer counts the amount of time elapsed for an engine to consume 25, 50 or 100ml of fuel. Figure 3.4 shows that the fuel timer’s external output was a voltage corresponding to nominally 4.8v when counting and 0v when not.

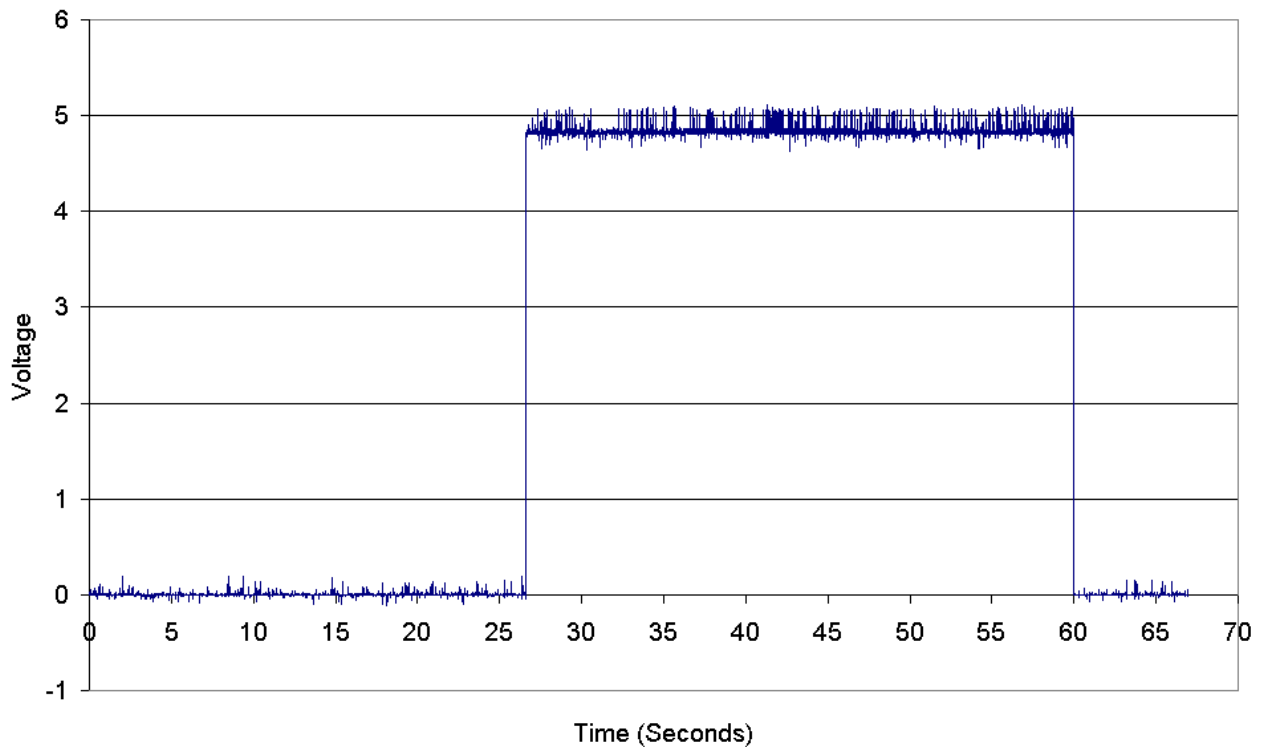


Figure 3.4 – Fuel timer voltage output

3.3.7 NTK Air / Fuel Ratio Meter

The NTK AFR meter has a configurable range for its external output. The output of the NTK was determined as 5V when reading the unit's maximum AFR of 33.30. Assuming a linear calibration with 0V as zero AFR, the calibration is 6.66 AFR/V. This was confirmed by the good correlation between the AFR output on the NTK box and the voltage output when the engine was running. Calibrating the NTK in a method similar to that used with the dynamometer outputs would be preferable, however this would require a programmable fuel system on the engine to enable the fuelling to be modified.

3.4 Real time Software Development

3.4.1 Introduction

Once the hardware had been put in place, calibrated and validated it was possible to develop software to calculate and display various engine parameters in real time. A screenshot of the final software is shown in figure 3.5.

By using National Instruments' LabVIEW, software was developed that was compatible with a wide range of hardware including the National Instruments 6024E board fitted to the PC. LabVIEW provides examples of triggered data acquisition using an external clock source. This provided the means to trigger an acquisition using the TDC marker and acquire data using the PLL output as an external clock source.

A number of requirements were identified for the software:

- Acquire cylinder pressure data in real time
- Acquire engine speed, torque and throttle demand from the dynamometer controller
- Acquire AFR from the NTK Air Fuel Ratio meter
- Acquire inlet manifold pressure from the manifold pressure transducer
- Time fuel consumption timer output
- Calculate power, thermal efficiency, volumetric efficiency, BSFC, BMEP, IMEP, peak pressure and fuel flow rate
- Save snapshots of raw and calculated parameters to file

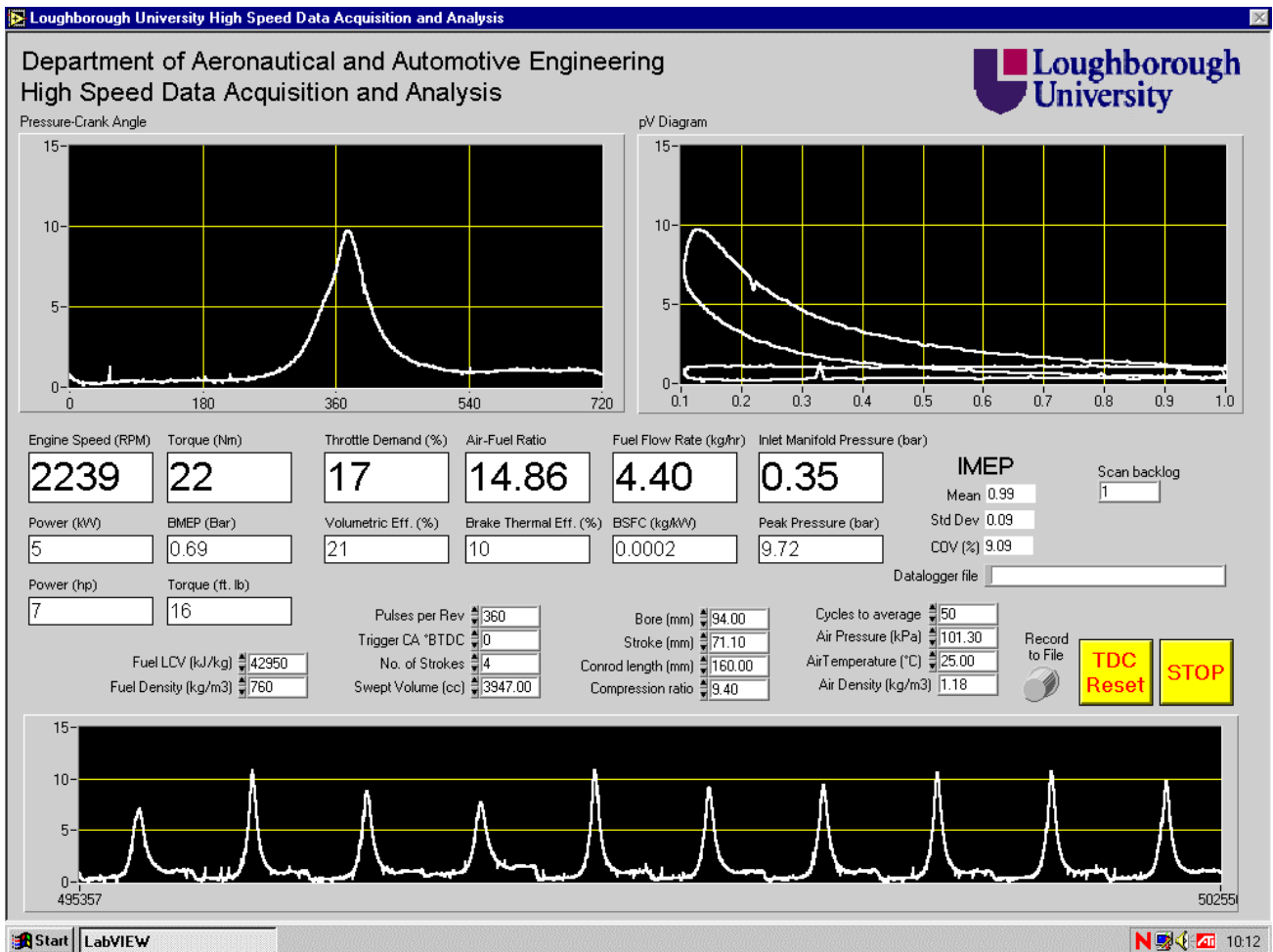


Figure 3.5 – Real time acquisition and analysis screenshot

3.4.2 Calculated parameters

The formulas used in the calculation of engine performance parameters are outlined below.

Torque

Torque is measured from the engine dynamometer itself. However, the conversion from Newton metres to foot-pounds uses the conversion factor:

$$T_{lb-ft} = 0.73756214836955 \times T_{Nm} \quad \text{(Equation 3.2)}$$

Brake Power

$$P_{brake} = \omega.T = 2\pi.N.T \quad \text{(Equation 3.3)}$$

where

P_{brake} is the brake power in kilo Watts
 ω is the engine speed in radians/sec
 T is the engine torque in Newton metres
 N is the engine speed in revolutions per second

The conversion between kilo Watts to brake horse power is:

$$P_{bhp} = 1.3410218586563 \times P_{kW} \quad (\text{Equation 3.4})$$

Thermal efficiency

$$\eta_{th} = \frac{P_{brake}}{N_c \cdot \dot{m}_{fuel} \cdot LCV} \quad (\text{Equation 3.5})$$

where

η_{th} is the thermal efficiency
 \dot{m}_{air} is the mass flow rate of air into the engine in kilograms per second
 N_c is the engine speed in cycles per second (N/2 for a four stroke engine)
 LCV is the lower calorific value of the fuel in kilo Joules per kilogram

Volumetric efficiency

$$\eta_v = \frac{\dot{m}_{air}}{\rho_{air} \cdot V_{swept} \cdot N_c} \quad (\text{Equation 3.6})$$

where

η_v is the volumetric efficiency
 ρ_{air} is air density in kilograms per cubic metre
 V_{swept} is the swept volume of the engine in cubic metres

In this case mass flow rate of air is not measured, however it can be calculated from the mass flow rate of fuel and the air-fuel ratio:

$$\eta_v = \frac{\dot{m}_{fuel} \cdot AFR}{\rho_{air} \cdot V_{swept} \cdot N_c} \quad (\text{Equation 3.7})$$

where

\dot{m}_{fuel} is the mass flow rate of fuel in kilograms per cubic metre
 AFR is the air fuel ratio

Air density is calculated from ambient temperature and pressure conditions using equation 3.8.

$$\rho_{air} = \frac{p_{air}}{R.T_{air}} \quad \text{(Equation 3.8)}$$

where

p_{air} is the ambient air pressure in Pascals
 R is the characteristic gas constant (287 J/kg K for air)
 T_{air} is the ambient air temperature in Kelvin

Brake specific fuel consumption (BSFC)

The specific fuel consumption is the fuel flow rate per unit power output. It is a measure of how efficiently an engine is using the fuel supplied to produce work.

$$bsfc = \frac{\dot{m}_{fuel} \cdot N_c}{P_{brake}} \quad \text{(Equation 3.9)}$$

Brake mean effective pressure (BMEP)

Whilst torque measures a particular engines ability to do work, it depends on engine size. A more useful relative engine performance measure is obtained by dividing the work per cycle by the cylinder volume displaced per cycle. Because the maximum brake mean effective pressure is well established, and effectively constant over a wide range of engine sizes, the engine designed can assess how effectively the engine's displacement has been utilised.

$$bmep = \frac{T \cdot 4 \cdot \pi}{V_s} \quad \text{(Equation 3.10)}$$

Fuel flow rate

Fuel flow rate is calculated from the time to consume 25ml of fuel.

$$\dot{m}_{fuel} = \frac{M \times 10^{-6}}{t} \times \rho_{fuel} \quad \text{(Equation 3.11)}$$

where

M is the volume of fuel measured in millilitres
 t is the time for M millilitres of fuel to be consumed in seconds
 ρ_{fuel} is the density of the fuel consumed in kilograms per cubic metre

Because the fuel timer takes a relatively large amount of time to count the amount of fuel used, the calculated fuel flow rate will not be correct at a particular engine point until the acquisition software has seen a ramp from zero to 5 volts and a subsequent ramp from 5 to

zero volts. This limitation can be minimised by resetting the fuel timer once a new engine speed-load point has been set.

Cylinder pressure analysis

Because the acquisition software sees two TDC pulses per engine cycle it necessary to include a TDC Reset button on the screen. If the acquisition starts with peak pressure occurring at the beginning/end of the pressure-crank angle graph then the TDC Reset button can be used to reset the acquisition until peak pressure occurs around the 360 degree mark.

Due to the real time nature of the data acquisition some simplifications must be made to ensure computational efficiency. Therefore absolute cylinder pressure is determined by setting the pressure at the bottom of the induction stroke to that of the inlet manifold pressure.

This has the advantage that it is quick and simple; however tuning effects from the inlet system will mean inaccuracies at higher engine speeds.

Indicated mean effective pressure (IMEP) is calculated in real time using the formula:

$$imep = \sum_{i=0}^{719} p_i \cdot \frac{dV}{V} \quad (\text{Equation 3.12})$$

By calculating the values of $\frac{dV}{V}$ before acquisition begins, this provides a computationally efficient method of determining net imep.

A running average is kept over a user specified number of engine cycles and the mean, standard deviation and coefficient of variance calculated. This provides an indication of the cyclic variability of the engines combustion process.

3.4.3 Validation of Calculated Parameters

In order to validate the parameters calculated by the LabVIEW software, engine data was recorded at a range of engine speeds between 1000 and 5000 RPM. This data could then be graphed, such as the throttle demand map in figure 3.6.

This data was then compared with published data to ensure the trends and order of data was comparable. This increased confidence that the data provide by the system was valid.

In order to provide confidence that the system was acquiring repeatable data, two full load torque curves were measured on differing days. These were plotted together in figure 3.7 and show good agreement between the two days. Slight differences are expected due to differing ambient air temperature and pressure.

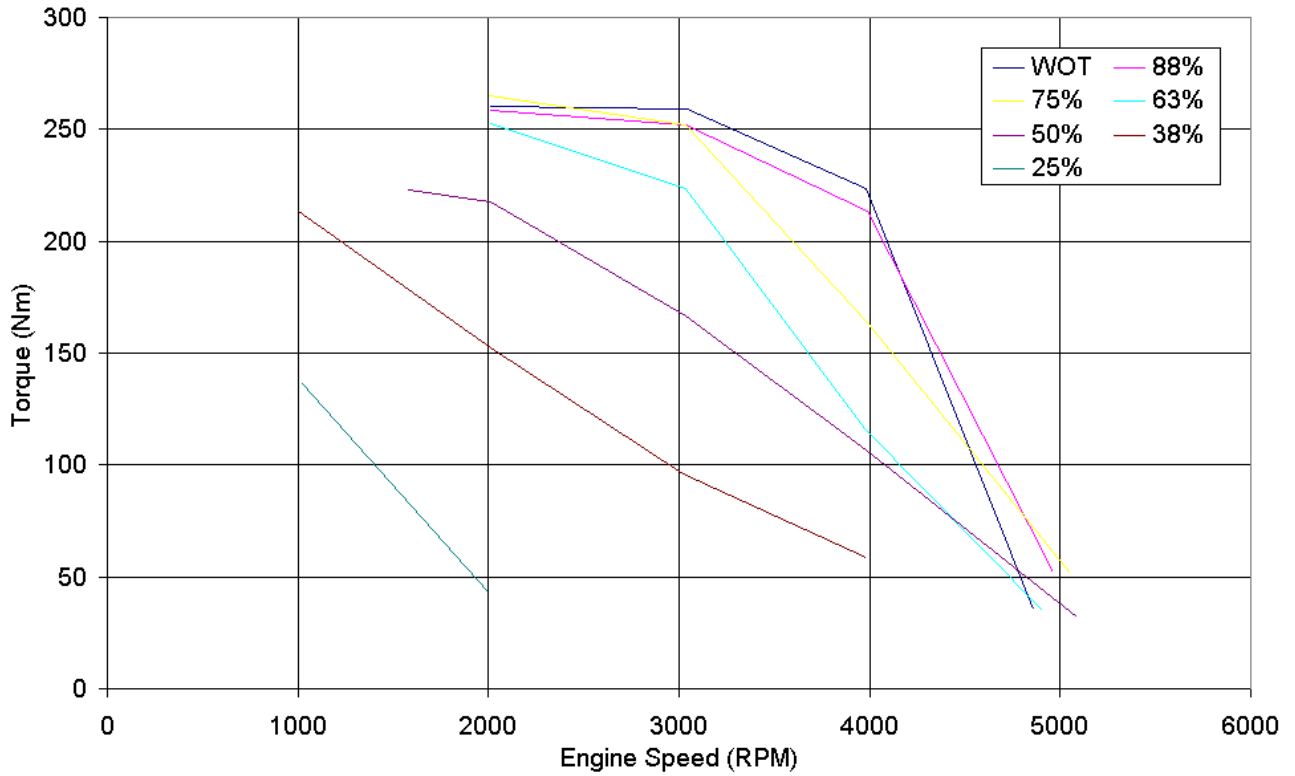


Figure 3.6 – Rover V8 throttle demand map

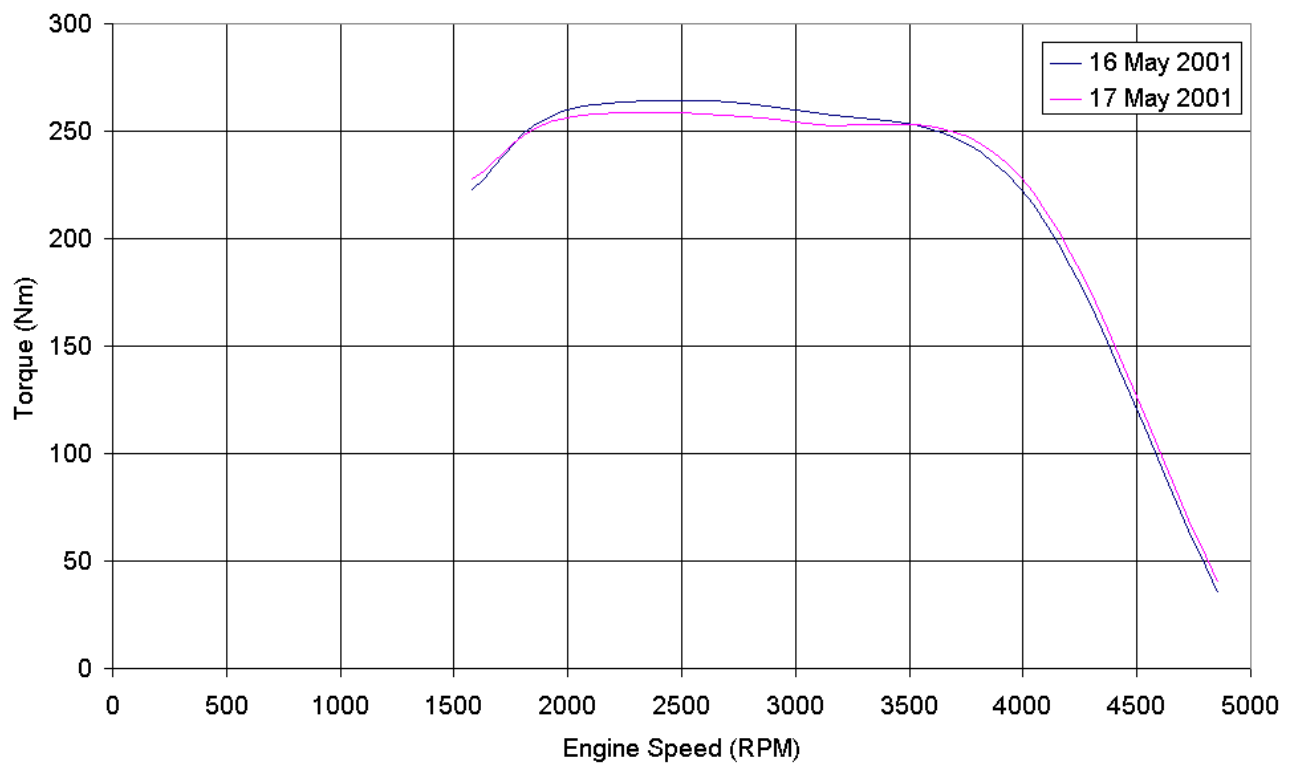


Figure 3.7 – Rover V8 full load torque curves

4.0 Data Analysis

4.1 Introduction

The software developed to analyse recorded cylinder pressure data is programmed in C++ and provides processing and analysis functions that are required for combustion analysis. The following chapter will discuss the features and limitations of the implemented software and the methods that have been chosen.

4.2 Analysis Formulas and Methodologies

4.2.1 Loading Data

When loading raw cylinder pressure data for analysis there are several factors that must be considered before the data is ready to be used.

TDC Error

Despite the best efforts to set the TDC trigger at the correct position, as discussed in section 3.3, it is not always possible. Therefore the analysis software is capable of adjusting the recorded TDC by way of a TDC error factor. In order to ensure enough data is recorded an extra engine cycle is recorded to ensure the requested number of engine cycles are available for analysis.

Determining the TDC error is available through two primary methods; Firstly, through the recording and analysis of pressure data from a motored engine; Secondly, through the use of a microwave or proximity probe to determine actual TDC.

Figure 4.1 shows in-cylinder pressure data recorded from a motoring engine. The location of peak pressure occurs slightly before TDC, which is expected due to the effects of heat transfer to the cylinder walls and gas blow by.

From the cylinder pressure data the thermodynamic loss angles (TLA) for each cycle can be calculated, as shown in figure 4.2. The location of peak pressure, θ_{max} , is determined between the range of 260 and 460 degrees, allowing for errors in TDC of up to ± 100 degrees. Through one-degree steps between 14 and 4 degrees before θ_{max} the corresponding pressure after θ_{max} is located. The mean crank angle between these two points is averaged over the ten-degree range giving the TLA for that engine cycle. This method is similar to that used by AVL³⁰ and MACAO³¹.

For an average passenger gasoline engine a TLA of between 0.7 and 1.3 degrees would be expected³⁰. As can be seen from figure 4.2, the Rover V8 engine has a TLA of around four degrees. It would therefore be reasonable to conclude a TDC error of three degrees. Because the TLA error is positive the first 717 degrees of engine data, rather than the first three degrees, should be discarded from subsequently acquired data.

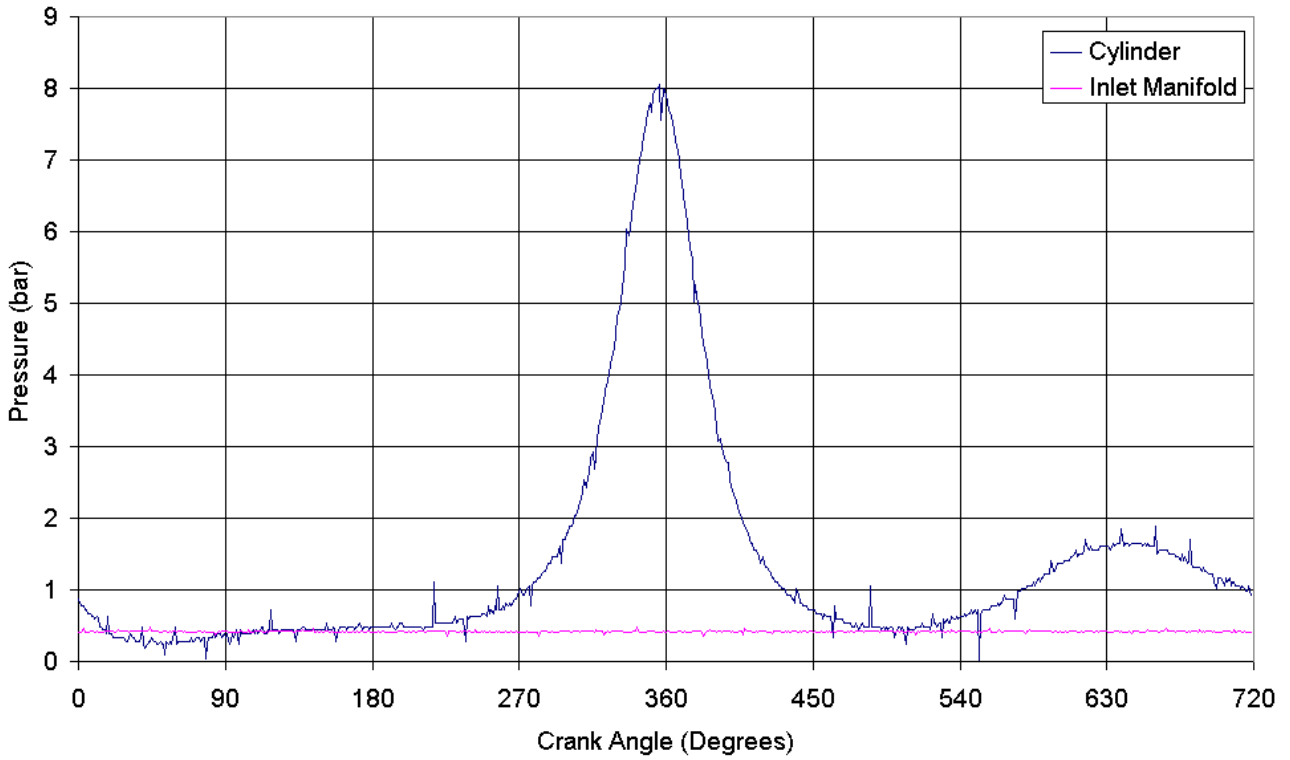


Figure 4.1 – Motored pressure data
(Rover V8 – Motored – 3200RPM)

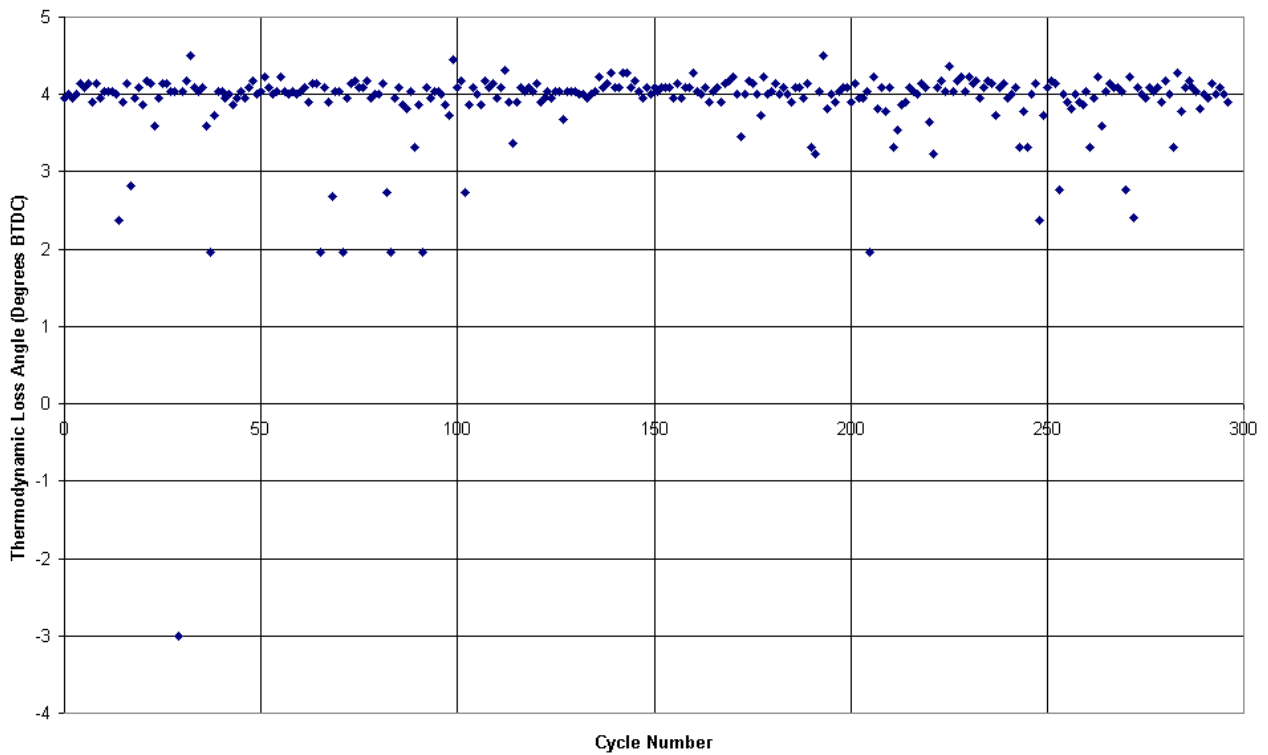


Figure 4.2 – Thermodynamic loss angle
(Rover V8 – Motored – 3200RPM)

A second method of analysing motored cylinder pressure data is presented by Tazerout et al³¹. They propose a process whereby graphs of temperature-entropy are plotted based on motored pressure data. At a TDC phase lag of 0.45° the characteristic looped shape of the graph disappears leaving an inverted parabola shape. The authors claim an accuracy within ± 0.1 degrees, however the value of 0.45° does appear to be derived from empirical simulation and observation and hence does not provide a method which could be used on all types and sizes of engine.

The method of determining TDC error most accurately is by way of using either a capacitance or microwave probe to measure actual piston lift. These devices are generally fitted into the spark plug or glow plug openings in the cylinder head and used in a motored condition to determine where TDC is located. This method, although most accurate, has the drawback that such equipment is costly to purchase, though it can be used quickly and effectively on a number of engines.

Incorrect TDC Trigger

As discussed in section 2.1, when acquiring four-stroke engine data, the TDC sensor is triggered at the end of both the compression and exhaust strokes. In order to overcome the problem of data acquisition occurring at the wrong TDC the following method has been developed:

Firstly, an extra 360 degrees of data is acquired on top of the requested number of engine cycles. This ensures that the requested number of whole engine cycles will be captured.

Secondly, the analysis software compares the acquired pressure data at the first and 360th degrees. If the pressure at 360 degrees, i.e. the end of the compression stroke, is greater than the first then the correct TDC trigger has been used to start acquisition. However, if the pressure is lower at the end of the compression stroke then acquisition has started at the incorrect TDC. Because an extra 360 degrees of data has been acquired at the end of the acquisition period, the first 360 degrees can be discarded.

If acquisition has started at the correct TDC then the final 360 degrees of extra data is ignored.

Channel angular offsets

The firing order of an engine dictates that whilst one cylinder is at a certain point in its thermodynamic cycle another cylinder will be a certain number of degrees advanced of this, as shown in figure 4.3. Generally acquisition is aligned to cylinder one and hence the other cylinders of the engine will be at varying stages of combustion when data is recorded.

The analysis software must account for this, ignoring a certain number of degrees of data depending on the offset between the recorded cylinder and the reference cylinder, as shown in figure 4.4.

Additionally, data that has been recorded such as inlet manifold pressure or block acceleration should be carefully referenced when referring to different cylinder cycle numbers. For example, for a four-cylinder engine with firing order 1-3-4-2, the inlet

manifold pressure referenced to cylinder three will be the inlet manifold pressure referenced to cylinder one at a crank angle 180 degrees later.

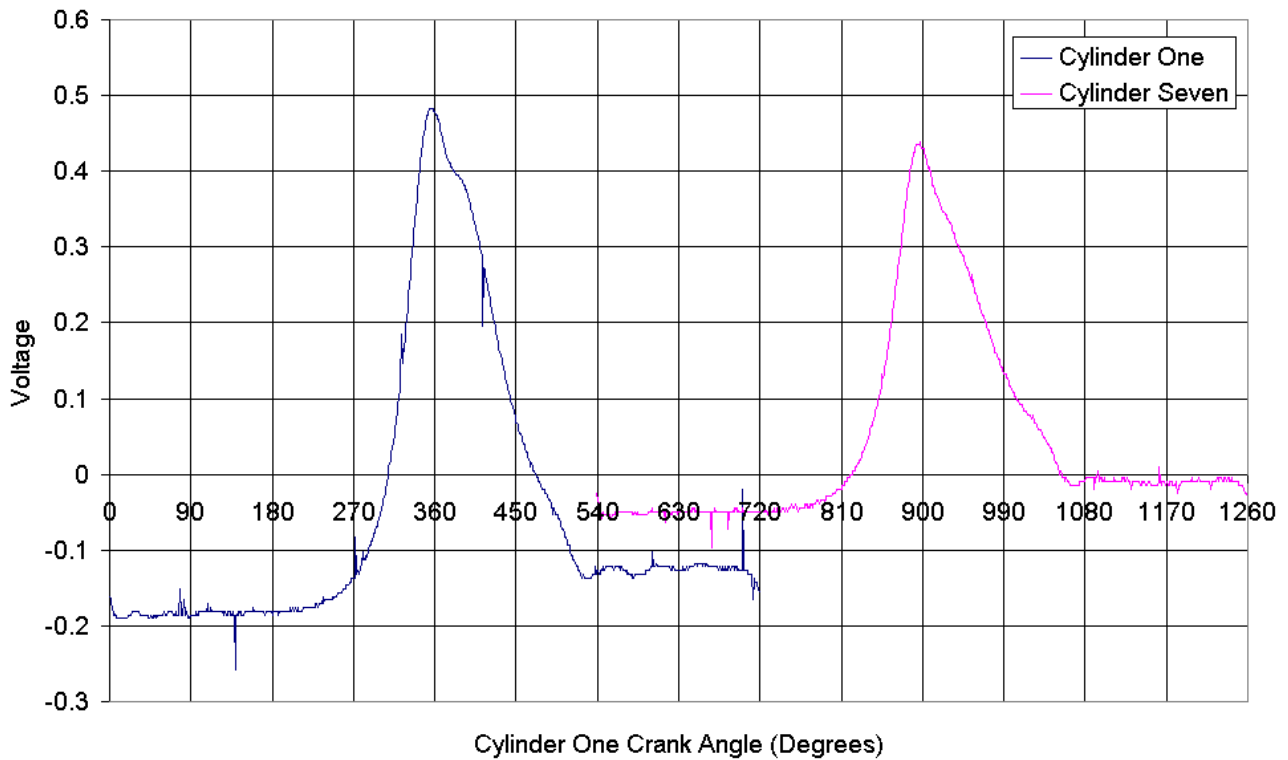


Figure 4.3 – Effects of firing order on acquired data (Rover V8 – Idle)

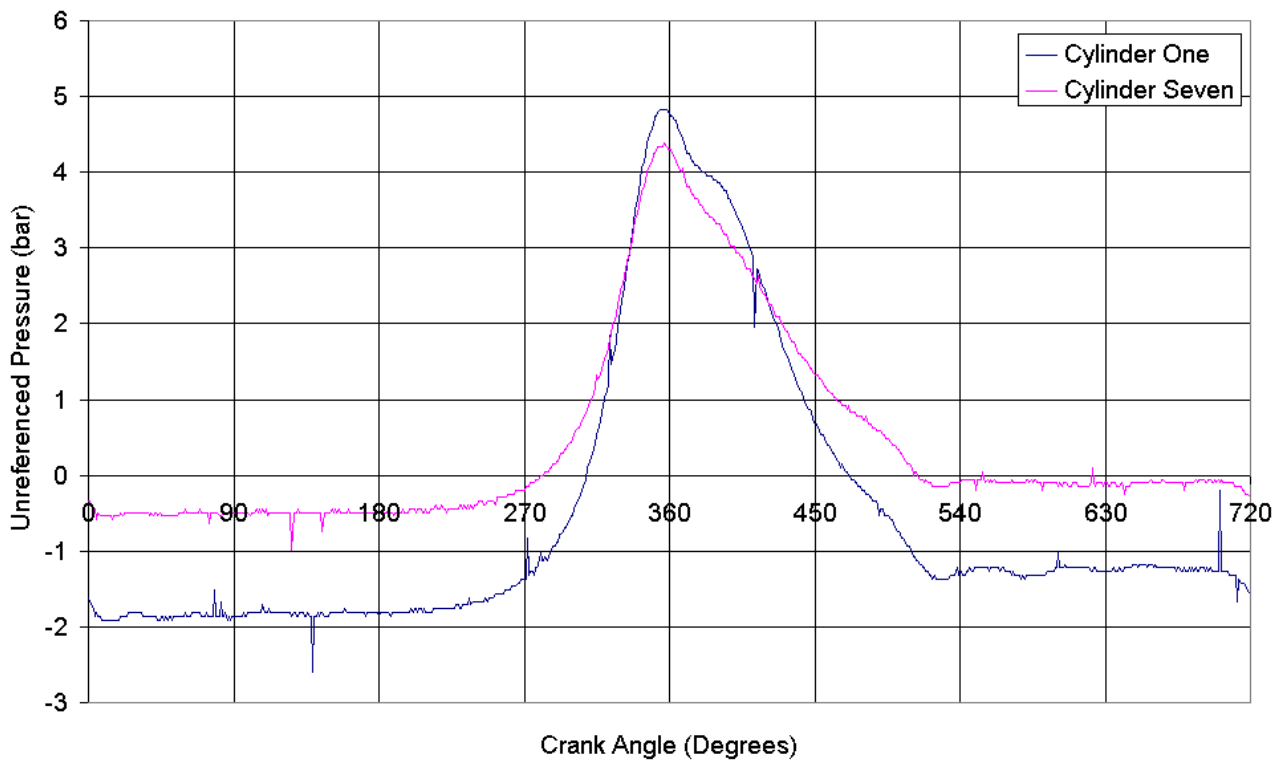


Figure 4.4 – Corrected crank angle referencing (Rover V8 – Idle)

4.2.2 Calculating Cylinder Volume

The purpose of the data acquisition system is to acquire engine data referenced to cylinder volume data. This is achieved by data acquisition occurring at known engine crank angles. To ensure accuracy the crank angle must be converted into cylinder volume using known engine geometry.

Heywood²¹, Stone⁸ and Lucas²² have all published formulas for obtaining cylinder volume from crank angle for a slider-crank mechanism (Equation 4.1).

$$V = V_C + \frac{\pi B^2}{4} (l + r - r \cdot \cos \theta - \sqrt{l^2 - r^2 \sin^2 \theta}) \quad (\text{Equation 4.1})$$

where

r is crank throw in metres

l is con rod length in metres

V_C is clearance volume at TDC in cubic metres

B is bore in metres

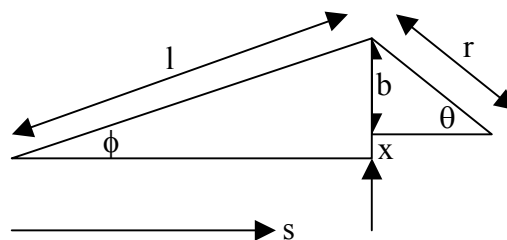
θ is crank angle measured from the beginning of the induction stroke in degrees

$$V_C = \frac{\pi B^2}{4} \frac{2r}{CR} \quad (\text{Equation 4.2})$$

where

CR is the compression ratio

However, this formula does not take into consideration the effect of wrist pin offset. In order to reduce piston 'slap' many pistons have a pin that is offset to the left, thrust side, when viewed from the front²⁹. Therefore, a formula has been developed from first principals to account for the changes in geometry this introduces.



$$V = V_C + \frac{\pi B^2}{4} s \quad (\text{Equation 4.3})$$

where

s is the displacement of the piston from TDC

$$s = l + r - r \cdot \cos \theta - l \cdot \cos \phi \quad (\text{Equation 4.4})$$

$$b = r \cdot \sin \theta \quad (\text{Equation 4.5})$$

$$b + x = l \cdot \sin \phi \quad (\text{Equation 4.6})$$

rearranging equations 4.5 and 4.6:

$$r \cdot \sin \theta = l \cdot \sin \phi - x \quad (\text{Equation 4.7})$$

rearranging gives:

$$\sin \phi = \frac{r \cdot \sin \theta + x}{l} \quad (\text{Equation 4.8})$$

substituting equation 4.8 into equation 4.4 gives:

$$s = l + r - r \cdot \cos \theta - l \cdot \cos \left(\sin^{-1} \left(\frac{r \cdot \sin \theta + x}{l} \right) \right) \quad (\text{Equation 4.9})$$

finally, substituted into equation 4.3 gives the equation of cylinder volume:

$$V = V_c + \frac{\pi B^2}{4} \left[l + r - r \cdot \cos \theta - l \cdot \cos \left(\sin^{-1} \left(\frac{r \cdot \sin \theta + x}{l} \right) \right) \right] \quad (\text{Equation 4.10})$$

where

x is the wrist pin offset in metres

Figure 4.5 shows that with identical engine geometry (zero wrist pin offset) the cylinder volumes calculated by equations 4.1 and 4.10 are identical.

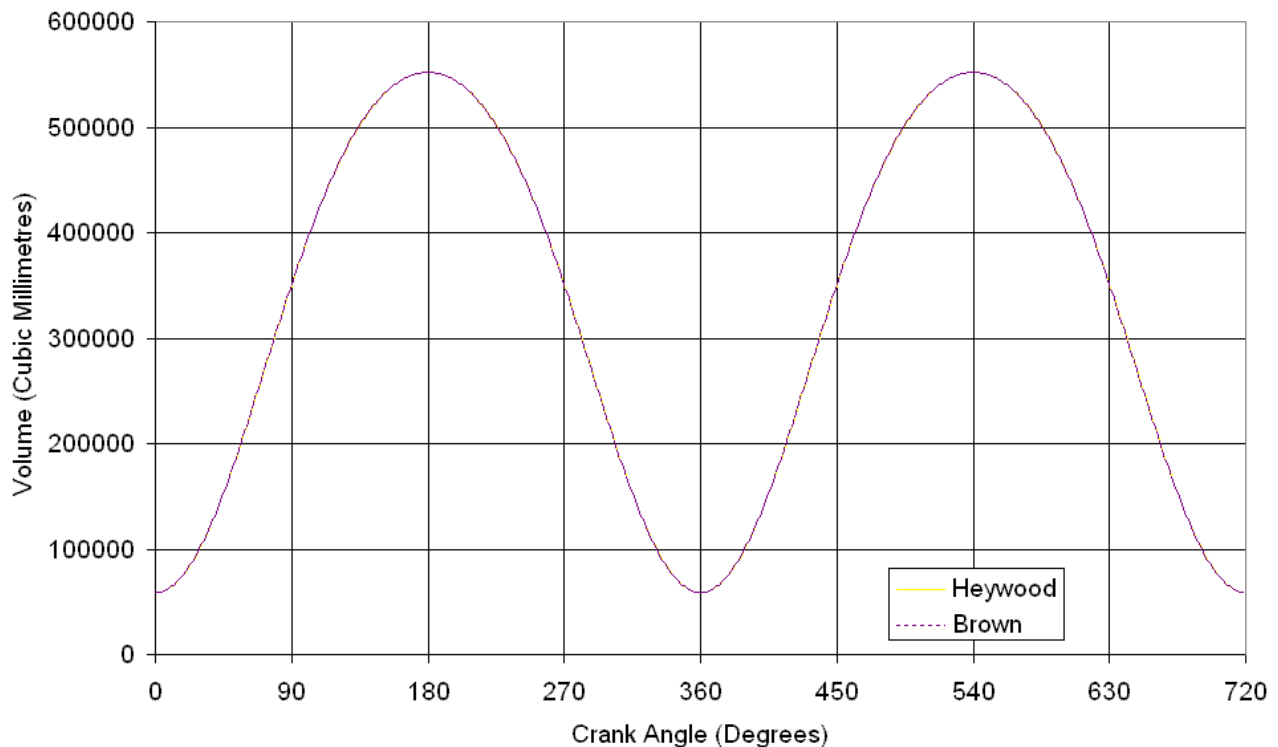


Figure 4.5 – Calculated cylinder volumes verses crank angle for Rover V8 engine

4.2.3 Absolute Pressure Correction

As has been discussed in section 2.2, the output of the piezoelectric pressure transducer is converted from electrical charge to a voltage using a charge amplifier. This acts as an integrating device of the charge over a set time period. This provides a pressure output that is relative rather than absolute.

Absolute pressure correction can be carried out using one of three processes:

Fixed pressure value at fixed crank angle – this is the simplest method available although it has the disadvantage that it is difficult to describe such a value or a suitable crank angle at which to apply a fixed value. Therefore this method, although available, is not recommended.

Equating manifold pressure to in-cylinder pressure at fixed crank angle – whilst this method may seem to be the best method available there is difficulty in determining what crank angle to equate inlet manifold and in-cylinder pressure. Due to the inertia effects of charge entering the cylinder the pressure at the end of the induction stroke can be above that of the inlet manifold. Also the inlet manifold pressure can fluctuate at higher engine speeds with the effects of resonating pressure waves in the inlet tracts.

Fitting the recorded compression pressure to a polytropic process – this method is favoured by many researchers. It has the benefit that no additional data need be recorded with the cylinder pressure data. However, it has the drawback that it can be difficult to select a polytropic index and which crank angle period to fit. The equation used is presented in the

literature review as equation 2.3. Douglas et al³² notes that this method is less suitable for two-stroke engines due to their increased cyclic variation.

Correcting absolute cylinder pressure on a cycle-by-cycle basis is also necessary due to drift of the piezoelectric pressure transducers. The correction will relieve intercycle drift, however intracycle drift can still be a problem, and hence analysing the amount of correction applied from one cycle to another can provide an indicator of excessive amounts of thermal shock.

In this report data has been corrected using a fixed polytropic index 1.32. This was chosen because it doesn't require the acquisition of extra data and when compared with intake manifold pressure, such as figure 4.6, compares well with fixing in-cylinder pressure to inlet manifold pressure at a given crank angle.

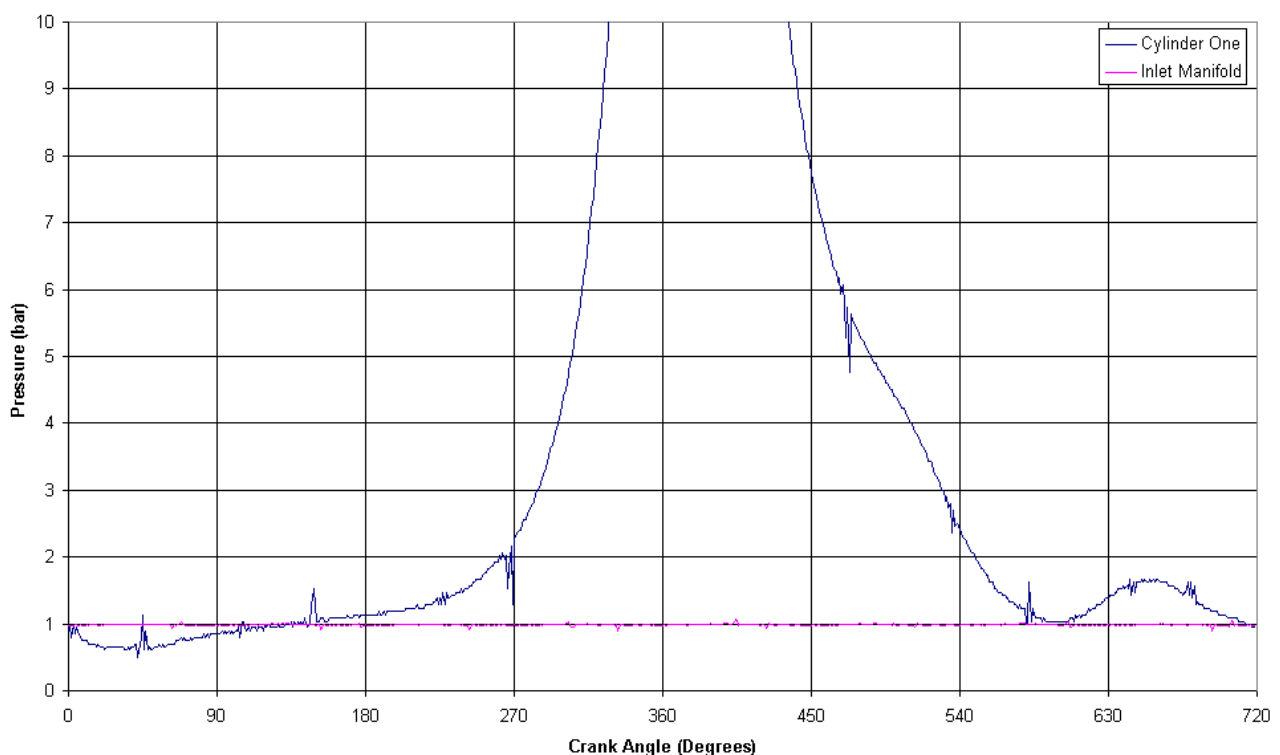


*Figure 4.6 – Corrected pressure curves using polytropic process
(Rover V8 – 3000RPM – WOT)*

4.2.4 Cylinder Pressure Analysis

Start and finish of combustion

The start of combustion is required for burn rates and heat release analysis. For a spark ignition engine this is the ignition timing and for a compression ignition engine it is the start of fuel injection.

The start of combustion can either be specified by the user or determined from a recorded channel, either low or high tension coil current for spark ignition engines or injector needle lift or fuel pressure in the case of compression ignition engines. In all cases start of

combustion is taken to be the crank angle with the greatest positive rate of change of the measured parameter whether it be voltage, current, displacement or pressure.

The estimated end of combustion (EEOC) is required for determining the normalising value for mass fraction burned and for heat release analysis. There have been several methods suggested by researchers, but the most common is to determine the crank angle that provides a maximum value of equation 4.11.

$$x = p.V^{1.15} \quad (\text{Equation 4.11})$$

In order to reduce the effects of signal noise, the method is modified slightly to determine the crank angle that provides a maximum over a five-point summation of equation 4.11:

$$x = \sum_{i=\theta-2}^{i=\theta+2} p_i.V_i^{1.15} \quad (\text{Equation 4.12})$$

In order to ensure the end of combustion is not underestimated, ten degrees is added to the crank angle at which x reaches a maximum.

Mass Fraction Burned

Burn rate analysis is commonly used with spark ignition engines to determine the mass fraction burned. Rassweiler and Withrow¹³ developed a technique in 1938 that is still considered today to be both accurate and computationally efficient.

During combustion, the pressure rise, Δp , during a crank interval, $\Delta\theta$, is considered to consist of pressure rise due to combustion, Δp_c , and pressure change due to change in volume, Δp_v .

$$\Delta p = \Delta p_c + \Delta p_v \quad (\text{Equation 4.13})$$

As the crank angle increments from θ_i to θ_{i+1} the volume changes from V_i to V_{i+1} and the pressure from p_i to p_{i+1} . Assuming that the change in pressure due to volume change can be calculated from a polytropic process of constant k :

$$p_{i+1} - p_i = \Delta p_c + p_i \left[\left(\frac{V_i}{V_{i+1}} \right)^k - 1 \right] \quad (\text{Equation 4.14})$$

hence

$$\Delta p_c = p_{i+1} - p_i \left(\frac{V_i}{V_{i+1}} \right)^k \quad (\text{Equation 4.15})$$

Because the combustion process does not occur at constant volume, the pressure rise rate due to combustion is not directly proportional to the mass of fuel burned. Therefore the pressure rise due to combustion must be referenced to a datum volume, such as that at TDC, V_{tdc} .

$$\Delta p_c^* = \Delta p_c \frac{V_i}{V_{tdc}} \quad (\text{Equation 4.16})$$

By identifying the end of combustion and the number of crank angle intervals between start and finish of combustion, N , the mass fraction burned can be calculated:

$$mfb = \frac{\sum_0^i \Delta p_c^*}{\sum_0^N \Delta p_c^*} \quad (\text{Equation 4.17})$$

For the purpose of cycle-to-cycle analysis, the crank angle at which burn rate percentages of 1%, 2%, 5%, 10%, 50%, 90%, 95% and 99% mass fraction burned are determined. Additionally, the ignition delay and combustion duration are determined from mass fraction burned curves. The ignition delay is the crank angle between start of combustion and typically 1,2 or 5% mfb. Combustion duration is calculated as the crank angle between the end of the ignition delay and typically 90, 95 or 99% mfb. Determining small or large percentages such as 1 or 99% can be difficult due to the susceptibility of the calculation to the effects of noise with small pressure changes.

Figure 4.7 shows a typical mass fraction burned curve. The small negative dip is undesirable and is most probably caused by TDC error.

This method of calculating mass fraction burned was chosen because of its proven reliability and its widespread use. Also, research has shown that more complex models provide little additional accuracy.

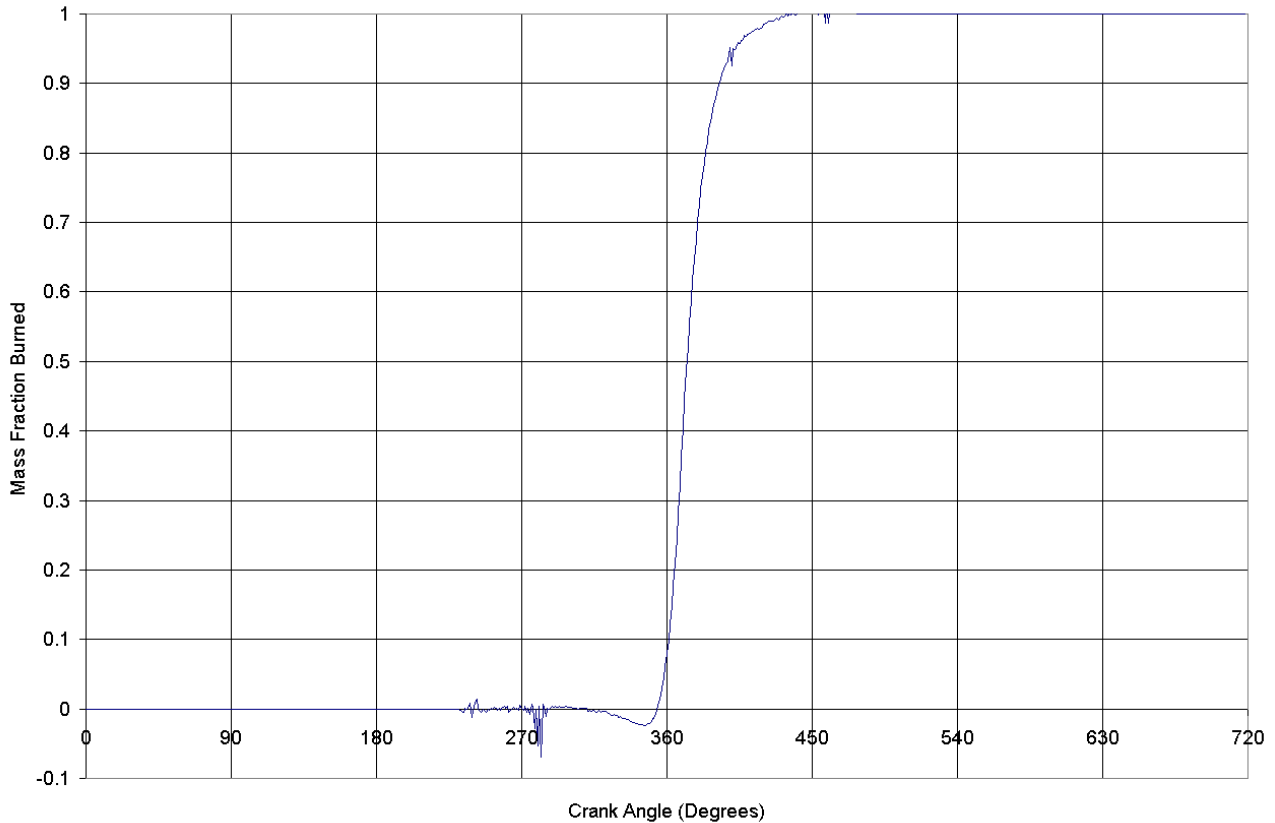


Figure 4.7 – Calculated mass fraction burned curve
(Rover V8 – 3000RPM – WOT)

Heat Release

Heat release analysis is generally applied to compression ignition engines, although there is no reason why it cannot be used in spark ignition applications. Heat release analysis computes how much heat would need to have been added to the cylinder contents, in order to produce the observed pressure variations⁸.

Using the first law of thermodynamics it can be shown^{6,8,21}:

$$\frac{dQ_{net}}{d\theta} = \frac{\gamma}{\gamma - 1} P \frac{dV}{d\theta} + \frac{1}{\gamma - 1} V \frac{dp}{d\theta} \quad \text{(Equation 4.18)}$$

where

γ is the ratio of specific heats

Q_{net} is the net heat release rate in Joules per degree

P is the in-cylinder pressure in Pascals

V is the in-cylinder volume in cubic metres

By taking into account the effects of heat transfer to the cylinder walls, the gross heat release can be calculated:

$$\frac{dQ_{gross}}{d\theta} = \frac{dQ_{net}}{d\theta} + \frac{dQ_{ht}}{d\theta} \quad (\text{Equation 4.19})$$

$$\frac{dQ_{ht}}{d\theta} = h(T - T_{wall}) \frac{dA}{d\theta} \quad (\text{Equation 4.20})$$

where

h is the heat transfer coefficient

T is the mean gas temperature in Kelvin, calculated from the equation of state ($pV=mRT$)

T_{wall} is the mean cylinder wall temperature in Kelvin

A is the instantaneous heat transfer surface area of the combustion chamber in cubic metres

Heat Transfer Coefficients

Over the years various papers have been published aiming to quantify the heat transfer coefficient to easily measured or derived engine parameters. Some of the most common functions used are implemented in the combustion analysis software and are presented below.

Hohenberg²³

$$h = 129.8V^{-0.06} p^{0.8} T^{-0.4} (\bar{v}_p + 1.4)^{0.8} \quad (\text{Equation 4.21})$$

Woschni²⁴

$$h = 129.8B^{-0.2} p^{0.8} T^{-0.53} \left(C_1 \bar{v}_p + C_2 \frac{V_s T_{ref}}{p_{ref} V_{ref}} (p - p_{motored}) \right)^{0.8} \quad (\text{Equation 4.22})$$

where

$C_1 = 6.18$ in scavenging period

$C_1 = 2.28$ in compression, combustion and expansion

$C_2 = 0$ in scavenging period and compression

$C_2 = 3.24 \times 10^{-3}$ in combustion and expansion

$C_2 = 6.22 \times 10^{-3}$ in combustion and expansion (IDI engines)⁸

Annand²⁵

$$h = \frac{a \cdot \lambda}{B} \text{Re}^{0.7} + c \frac{(T^4 - T_{wall}^4)}{T - T_{wall}} \quad (\text{Equation 4.23})$$

where

$$0.35 < a < 0.8$$

$c = 0$ during intake and compression

$c = 0.576\sigma$ for CI engine combustion and expansion

$c = 0.075\sigma$ for SI engine combustion and expansion

from Bosch²⁷ $\sigma = 5.67 \times 10^{-8} \text{ W}\cdot\text{m}^{-2}\cdot\text{K}^{-4}$

from Street et al²⁶

$$\text{Re} = \frac{V \cdot d \cdot \rho}{\mu} \quad (\text{Equation 4.24})$$

where

V is the mean velocity in the pipe (mean piston speed) in metres per second

d the characteristic length (engine bore) in metres

ρ is the density of the fluid in kilograms per cubic metres

μ is the dynamic fluid viscosity in kilograms per metre per second

Mean piston speed is calculated from engine speed. The software provides two sources of engine speed. The user can either specify it directly or if the engine speed channel has been recorded then the channel number can be specified and the speed averaged over the individual engine cycle periods. Recording engine speed has the benefit of accounting for the continually changing engine speed due to cycle-to-cycle variation of combustion.

$$V = 2 \cdot L \cdot N \quad (\text{Equation 4.25})$$

where

N is engine speed in revolutions per second

L is engine stroke in metres

$$\rho = \frac{p}{R \cdot T} \quad (\text{Equation 4.26})$$

Annand²⁵ approximates:

$$\lambda = \frac{C_p \cdot \mu}{0.7} \quad (\text{Equation 4.27})$$

from Brunt⁶:

$$C_p = \frac{R}{1 - \frac{1}{\gamma}} \quad (\text{Equation 4.28})$$

$$\gamma = 1.338 - 6.0 \times 10^{-5} \cdot T + 1.0 \times 10^{-8} \cdot T^2 \quad (\text{based on gasoline engine}) \quad (\text{Equation 4.29})$$

The following figures are published:

Brunt:

Annand:

$a=0.45$
 $R=288.8$

$\mu=4.702 \times 10^{-7} \cdot T^{0.645}$
 $R=241.1$

(Equation 4.30)

The validity of Annand's equation for dynamic fluid viscosity, equation 4.27, is compared in figure 4.8 to published figures. It is noted from the sources of the published values^{35,36,37} that μ does not vary significantly with pressure.

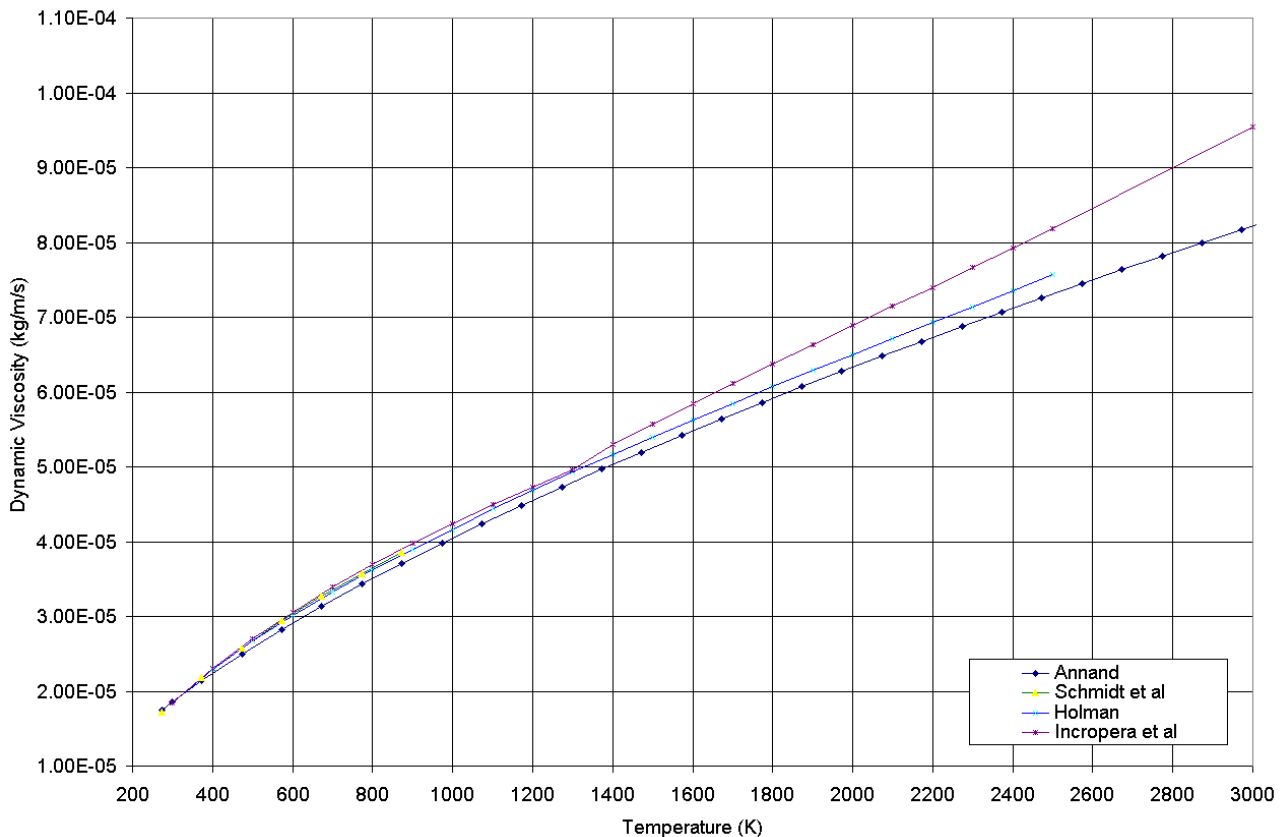


Figure 4.8 – Published values of the dynamic viscosity of air

It should be noted that the equations developed to calculate heat transfer coefficient are derived empirically from heat flux measurements. Therefore, the equations are only valid for the type and geometry from which they are derived.

Heat transfer coefficient formulas are used because it is impractical to derive accurate formula for every engine under investigation and because the differences between coefficients calculated by different formulae do not provide substantially different final results. The choice of which heat transfer coefficient to use, should be down to the particular application and whether data is being compared to data calculated using a particular method.

Mean Gas Temperature

The mean gas temperature is required for the calculation of heat release.

for a polytropic process²⁸

$$pV^n = \text{constant} \quad (\text{Equation 4.31})$$

$$\left(\frac{T_2}{T_1}\right) = \left(\frac{V_1}{V_2}\right)^{n-1} = \left(\frac{p_2}{p_1}\right)^{\frac{n-1}{n}} \quad (\text{Equation 4.32})$$

hence

$$T_2 = T_1 \left(\frac{V_1}{V_2}\right)^{n-1} = T_1 \left(\frac{p_2}{p_1}\right)^{\frac{n-1}{n}} \quad (\text{Equation 4.33})$$

for a known reference location, such as inlet valve closure:

$$p_{ref} \cdot V_{ref} = n \cdot R \cdot T_{ref} \quad (\text{Equation 4.34})$$

rearranging gives:

$$\frac{T_{ref}}{p_{ref} \cdot V_{ref}} = \frac{1}{n \cdot R} \quad (\text{Equation 4.35})$$

to calculate the temperature at an arbitrary position between inlet valve closure and exhaust valve opening:

$$T_{calc} = p_{calc} \cdot V_{calc} \cdot \frac{1}{n \cdot R} \quad (\text{Equation 4.36})$$

assuming n and R remain constant, equation 4.35 can be substituted into equation 4.36:

$$T_{calc} = p_{calc} \cdot V_{calc} \cdot \frac{T_{ref}}{p_{ref} \cdot V_{ref}} \quad (\text{Equation 4.37})$$

Rate of Pressure Rise

The rate of pressure rise is calculated using a simple numerical differentiation:

$$\frac{dp}{d\theta} = \frac{p_{i+1} - p_{i-1}}{\theta_{i+1} - \theta_{i-1}} \quad (\text{Equation 4.38})$$

High rates of pressure rise rate may help identify the occurrence of pre-ignition and knock³⁴; however, sampling resolution and signal noise can also give high rates of pressure rise. Therefore, good quality acquisition and filtering is required for this parameter to be useful.

IMEP

The combustion analysis software calculates indicated mean effective pressure using the following equation:

$$imep = \frac{\Delta\theta}{V_s} \sum p \cdot \frac{dV}{d\theta} \quad (\text{Equation 4.39})$$

This equation has been shown to be both computationally efficient and provide good robustness to coarse crank angle resolutions¹⁴.

Using the formula between 180 and 540 degrees provides the gross imep and, outside of this range, the pumping imep. The addition of these two parameters provides the net imep that includes the input of energy from combustion and the losses due to pumping.

Additionally, the pumping imep is split at atmospheric pressure between the upper and lower pumping loop imep. The upper pumping loop indicates the amount of energy required to propel the combustion products through the exhaust valve and piping system. The lower loop indicates the losses due to induction, including the throttling losses across the intake valve³³.

Peak Knocking Pressure

Knock analysis is important to understand how ignition timing leads to the occurrence of knock and how this understanding can be used in engine design and calibration.

The combustion analysis software uses two methods. The Checkel & Dale method is presented in equation 2.21 and Brunt et al in equation 2.23.

Because the engine under test was running a production level engine management system there was little scope to advance ignition timing to induce knock. Therefore, no knocking cylinder pressure data was available for analysis and validation of the implemented methods.

4.2.5 Cycle-by-cycle Analysis

Once data has been loaded into the analysis software, incorrect TDC and TDC error accounted for, and absolute pressure referencing carried out; the following parameters are calculated on a cycle-to-cycle basis:

- 1% MFB Angle
- 2% MFB Angle
- 5% MFB Angle
- 10% MFB Angle
- 50% MFB Angle
- 90% MFB Angle
- 95% MFB Angle
- 99% MFB Angle
- Engine Speed
- Estimated End of Combustion (EEOC)
- Gross IMEP
- Lower Pumping IMEP
- Maximum Burn Rate
- Maximum Burn Rate Crank Angle
- Maximum Heat Release Rate
- Maximum Heat Release Rate Crank Angle
- Maximum Pressure Rise Rate
- Maximum Pressure Rise Rate Crank Angle
- Maximum Pressure
- Maximum Pressure Crank Angle
- Maximum Mean Gas Temperature
- Maximum Mean Gas Temperature Crank Angle
- Peak Knocking Pressure
- Peak Knocking Pressure Crank Angle
- Expansion Polytropic Index
- Compression Polytropic Index
- Start of Combustion
- Thermodynamic Loss Angle
- Total Heat Release
- Upper Pumping IMEP
- Wiebe Functions (a and m)

4.2.6 Statistical Analysis

Statistical analysis of the parameters calculated on a cycle-by-cycle basis can provide much information about engine performance as opposed to studying individual engine cycles.

The analysis software calculates mean, maximum, minimum, standard deviation, coefficient of variance (CoV) and least normalised value (LNV) for each of the parameters calculated for each thermodynamic cycle.

The mean is calculated using:

$$\bar{p} = \frac{\sum_i^N p_i}{N} \quad \text{(Equation 4.40)}$$

where

N is the number of engine cycles recorded

\bar{p} is the mean of the calculated parameter

p_i is the parameter at cycle i

Standard deviation is calculated by:

$$\sigma = \sqrt{\frac{\sum_i^N (p_i - \bar{p})^2}{(N-1)}} \quad \text{(Equation 4.41)}$$

The coefficient of variance is calculated by:

$$CoV = \frac{\sigma}{\bar{p}_i} \quad \text{(Equation 4.42)}$$

The least normalised value is calculated by:

$$LNV = \frac{p_{min}}{\sigma} \quad \text{(Equation 4.43)}$$

where

p_{min} is the minimum parameter of all engine cycles recorded

4.2.7 Data Validation

Once analysis has been performed, various methods can be used to determine the validity of the acquired data. These methods aim to ensure that the user does not confuse poor data acquisition as poor engine performance.

By using the calculated mean, minimum, maximum and standard deviation of cycle-by-cycle parameters, upper and lower limits can be set on any parameter to indicate unusual engine behaviour. For example, a low polytropic expansion exponent, typically below unity, indicates combustion continuing to exhaust valve opening.

A second method of data validation is plotting calculated parameters against their cycle number. For example, figure 4.9 shows the location of peak pressure for 300 recorded engine cycles. If a problem had occurred with data acquisition, such as a noisy external clock source or too low an acquisition rate, the crank angle of peak pressure would show a slow but definite drop off as the cycle number increased. Figure 4.9 shows no such trend, thereby indicating correct timing over the entire acquisition.

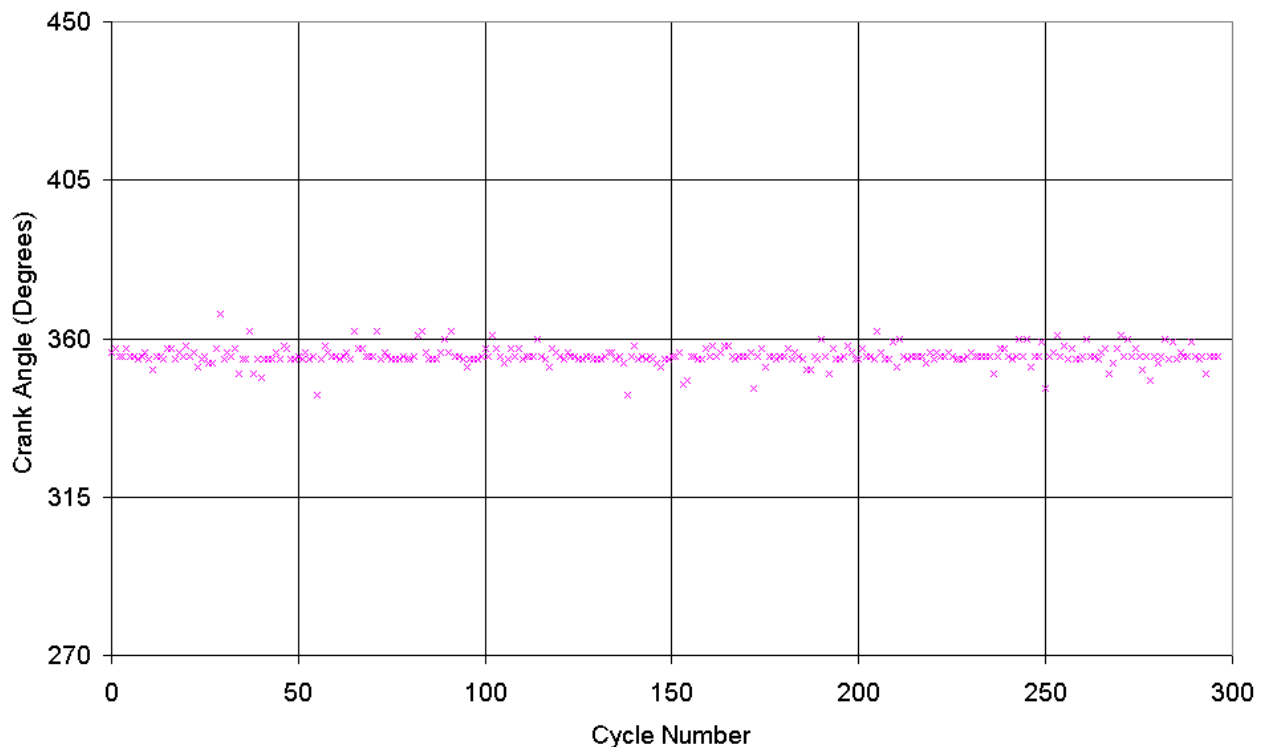


*Figure 4.9 – Location of peak pressure
(Rover V8 – 3000RPM – WOT)*

4.3 Validation of implemented system

In order to ensure the implementation of the presented formulas is valid, comparisons with published figures has been made. The purpose of these comparisons is to show that the general shape and magnitude of calculated and published figures are similar.

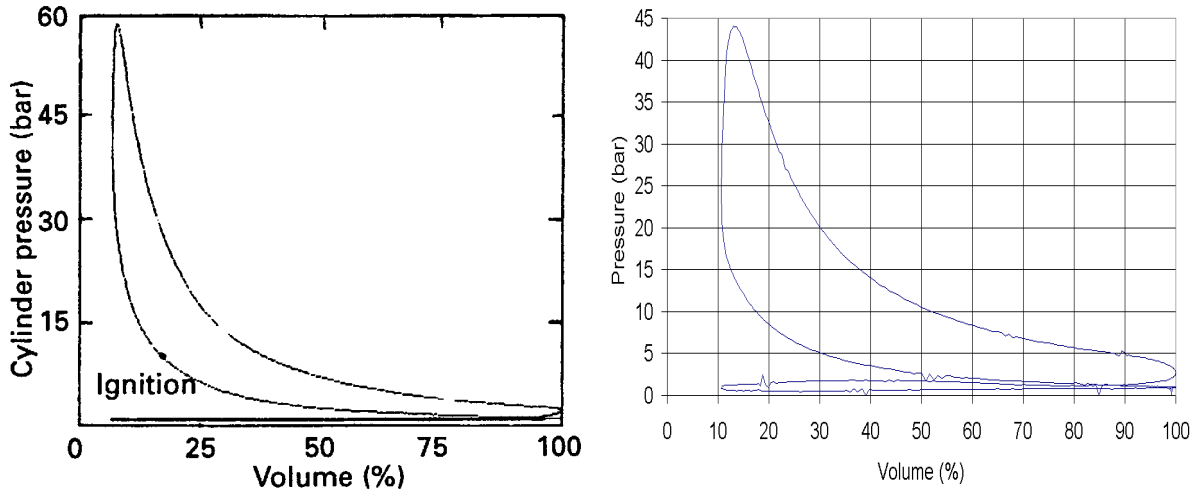


Figure 4.10 – pV Diagram, published figure⁸ (left) and analysis output (right)

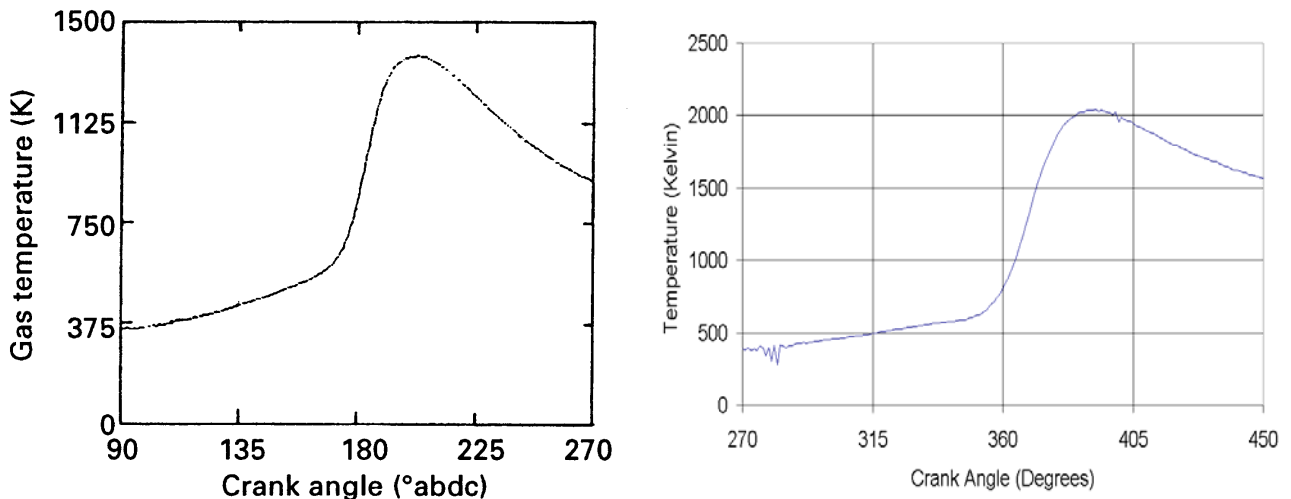


Figure 4.11 – Mean gas temperature, published figure⁸ (left) and analysis output (right)

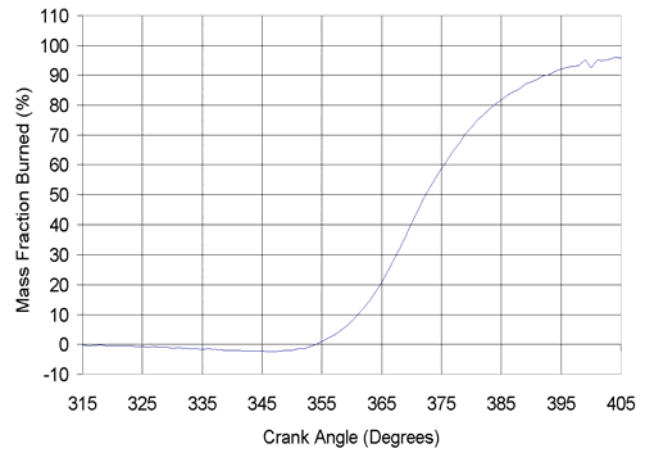
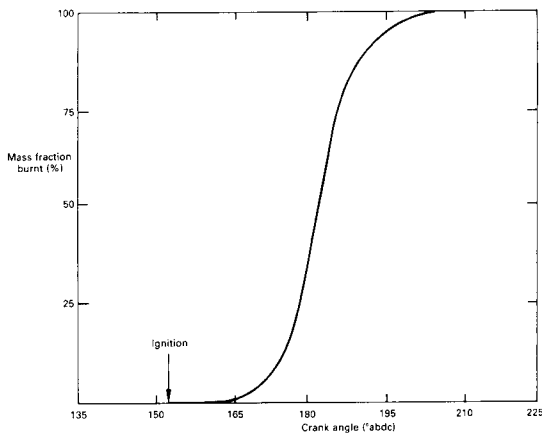


Figure 4.12 – Mass fraction burned, published figure⁸ (left) and analysis output (right)

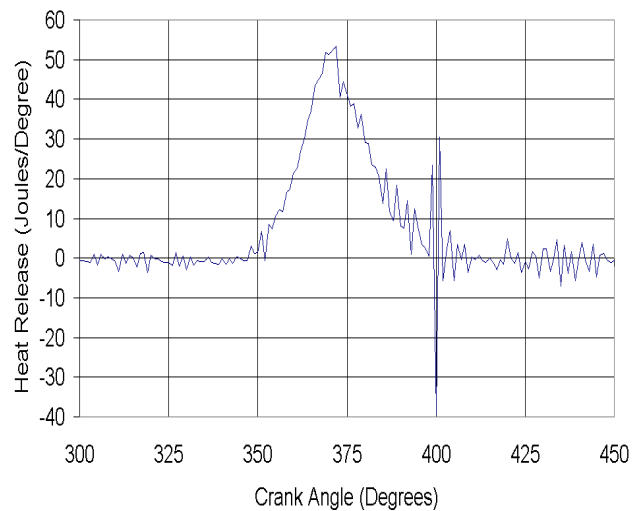
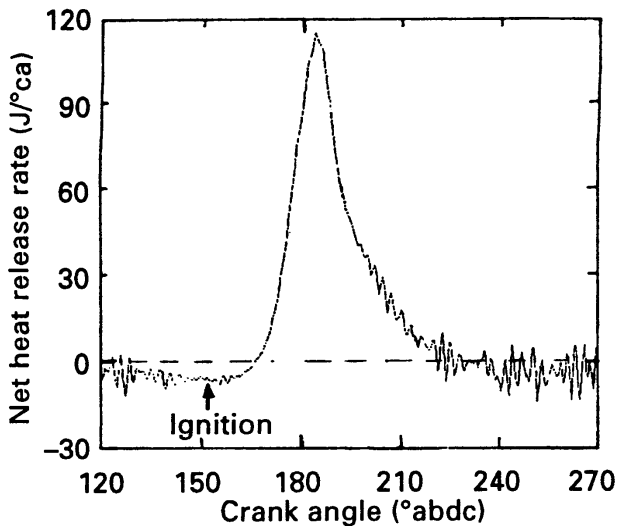


Figure 4.13 – Net heat release, published figure⁸ (left) and analysis output (right)

Figures 4.10 through 4.13 show good agreement between published and calculated values. The mass fraction burned curve shows slower combustion occurring and this is confirmed by the lower rates of heat release. Signal noise around the 400-degree mark can be seen to have little effect on the calculated mean gas temperature and mass fraction burned. However, it makes a significant spike in the heat release calculations, although the effect of this on the total heat release of the cycle should be minimal due to the summing effect.

5.0 Future Improvements

5.1 Introduction

Over the course of this project several areas of improvement or extension have been identified. The purpose of this project was to build a firm base on to which further work can be carried out to increase the usefulness and accuracy of engine acquired data.

The following outlines possibilities for future investigation and includes preliminary findings and ideas developed as part of this project.

5.2 Data Acquisition

5.2.1 Crank angle encoder

TDC determination from motored engine data and knock phenomenon investigation require a more accurate crank angle encoder than that which is currently provided with the flywheel-based system. During the course of the project an AVL crank encoder with high, 0.1 degree, resolution was located. This would require the fabrication of a solid mounting bracket for the front of the engine and connection to the end of the engine crankshaft. An example of how to achieve this can be seen on the departments' optical research engine.

5.2.2 Spark-plug pressure transducer

The use of the Rover V8 engine throughout this project was dictated by the fact that the pressure transducers available are designed for fitment into the combustion chamber of specially modified cylinder heads, such as the Rover's. If the department were to purchase additional pressure transducers then spark plug pressure transducers would allow fitment to a multitude of different spark ignition engines. This also relieves the time, cost and difficulty of removal, machining and refit of cylinder heads to engines requiring analysis.

5.2.3 Accurate TDC determination

With more accurate crank angle encoders, a more accurate determination of the TDC error from motored pressure data analysis can be performed. The current error estimation is in the region of $3^{\circ} \pm 0.5^{\circ}$. It has been identified that for accurate data analysis and error of around $\pm 0.1^{\circ}$ for compression ignition engines and $\pm 0.3^{\circ}$ for spark ignition engines is required. Clearly the current estimate does not provide the necessary accuracy to provide high quality data analysis.

5.2.4 Fast response inlet / exhaust value pressure transducer

Recording the pressure fluctuations in inlet and exhaust tracts provides important information with regards to gas tuning effects and how these affect cylinder filling and scavenging. This is important in the investigation and design of camshafts and inlet and exhaust geometry, especially so in the case of variable systems.

The fitment of pressure transducers that have sufficiently high resolution and response to small pressure changes would allow such work to be carried out. Acquisition of such data

would require no modifications to the current hardware or software and would allow correlation between the pressures in the inlet, cylinder and exhaust ports at given stages of the engine cycle.

5.2.5 Start of combustion

As has been discussed in section 4.2.4, determining the start of combustion is important for the calculation of burn rates and heat release. A method has been implemented that determines the start of combustion from the peak rise rate of a recorded data channel. The type of data depends on engine type and includes high and low tension ignition voltage, shown in figure 5.1, or injector needle lift or fuel line pressure, as shown in figure 5.2.

However, because suitable data was not available, such functionality has not been fully tested and validated. The easiest type of data to measure would be high-tension spark voltage. This is the voltage induced in a wire wrapped around one of the high-tension ignition leads. This would require measures to ensure excessive voltage did not overload the data acquisition hardware.

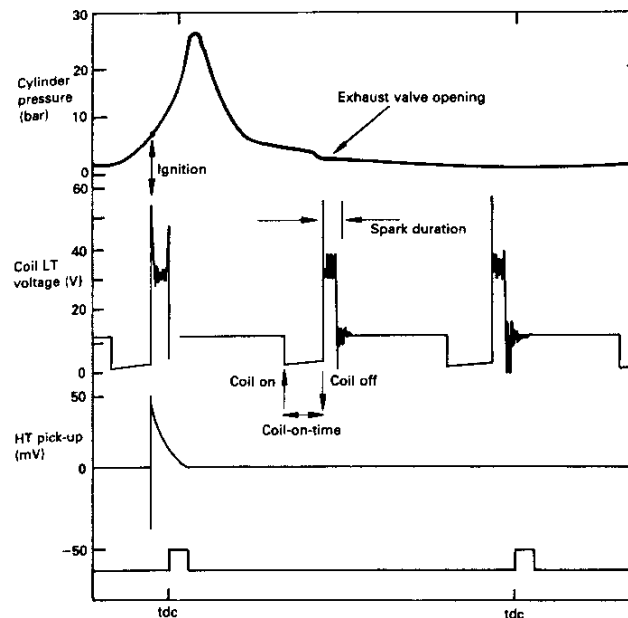


Figure 5.1 – Recorded ignition voltage as an indication of start of combustion⁸

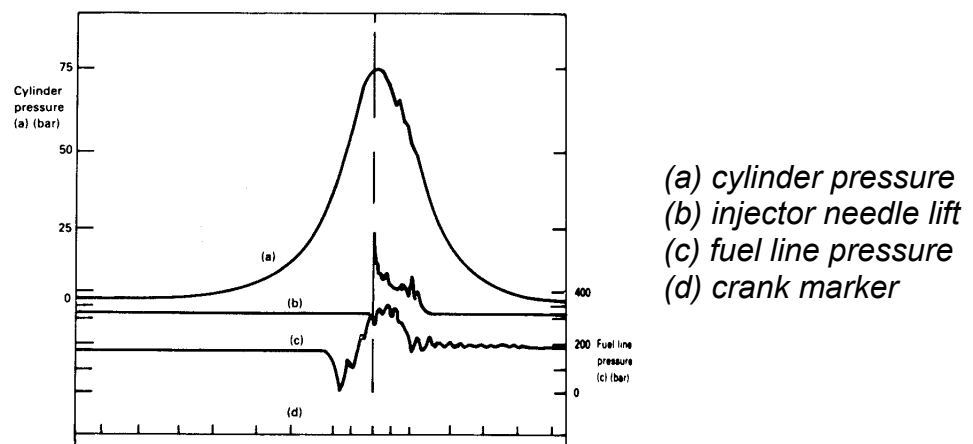


Figure 5.2 – Recorded fuel pressure as an indication of start of combustion⁸

5.2.6 Real time processing

The absolute pressure correction used for real time analysis is a simple equating of induction BDC in-cylinder pressure to that of the inlet manifold. This has its limitations as discussed previously; therefore it would be preferable to fix each engine cycle to a specified polytropic index in real time.

This would increase the accuracy of peak pressure calculations; although it has been identified in the literature review that absolute pressure correction has no effect on IMEP values.

The effects of TDC error on IMEP have been identified in the literature review. Therefore it would be beneficial to allow this error to be taken into account for the analysis of real time data. This would be more difficult than the process used for offline analysis as the acquisition hardware is programmed for triggering using the TDC sensor.

A possible solution is to acquire TDC data when real time analysis is started and wait for a specified number of crank angles after the TDC marker has passed before beginning a non-triggered acquisition using the existing PLL external clock source.

5.2.7 Dynamometer Control

The user currently controls the dynamometer manually. It would be possible to use the analogue voltage outputs of the acquisition card to control the throttle position and dynamometer load. This would, for example, allow the automation of full load power runs. However, this automation would also require the acquisition of extra data such as oil temperature and pressure to ensure any problems with the engine were detected and the engine shutdown.

5.3 Data Analysis

5.3.1 Filtering

The effects of signal noise can have a detrimental effect on the validity of calculated parameters. In addition to the careful cleaning and placement of equipment when acquiring raw data, filtering can be used to minimise signal noise.

There are two types of filters, analogue and digital. Both types should be frequency selective, that is, let frequency components over a given frequency range, the passband, pass through undistorted while other frequencies, the stopband, are completely cut off.

Analogue filters use electrical components, such as resistors and capacitors, to filter data as the data is collected. This has the advantage that it is transparent to the user and the data recorded requires no further processing. Depending on the speed of response of the analogue circuit, a small phase lag can be introduced. Digital filtering is applied after data has been recorded. This has the advantage that no external filters are required, reducing hardware costs. Digital filters have the advantage that the user can apply different filters and investigate how they affect the recorded data. Digital filters generally introduce a phase lag but this can be removed by processing the data in both the forwards and backwards directions. For example, recorded pressure data should be filtered from 0 through 720 degrees and then the filtered output re-filtered from 720 to 0 degrees.

The current software has no filtering capabilities, however it is a simple matter to add this. It would also require a filter designer in order to determine the filter coefficients. A second order Butterworth filter has been suggested by Brunt³, and textbooks relating to Digital Signal Processing, DSP, have details of how to design such filters.

No analogue filtering was used to collect data, as the Kistler charge amplifiers' built in filters were turned off, however an area of future research could be conducted on the effects that these filters have on the quality of acquired data.

5.3.2 Knock analysis

Knock analysis is important in determining the suitability of engine's knock sensor location to knock control³⁸. Comparisons can be made between the knock intensity calculated from cylinder pressure measurements and the accelerations measured at the engine knock boss. Additionally, the fast Fourier transform (FFT) of accelerometer data can be used to determine the centre frequencies, typically in the range 6 – 20 kHz, used in the calibration of knock control systems.

Therefore, the software requires the ability to perform FFT on recorded data. There are various published pieces of code that will perform FFT calculations quickly and efficiently such as `fftw` (www.fftw.org).

5.3.3 Graphical Front End

Although the functionality of a software package dictates what the ultimate capabilities are, a simple and effect user interface can enable quicker and more effective use of the software and its features. Therefore, designing a simple yet powerful interface for the software to run in the Microsoft Windows environment would be beneficial.

Such software could import data files, run the analysis and then be used to display the analysis directly, rather than loading and charting in a spreadsheet, such as Microsoft Excel.

Such software should be capable of displaying parameters against each other such as cylinder pressure and crank angle or by displaying parameters such as peak cylinder pressure for all engine cycles recorded.

5.3.4 Importation of industry standard files

It is important with any piece of software to share data. Within the combustion analysis field two formats for saving combustion data are commonly used, the AVL I-file and the Redline-CAS file format. Both of these file formats are publicly available and are included in the appendix.

5.3.5 Amount of fuel injected

If fuel line pressure and fuel injector needle lift is recorded then the orifice flow equation can be used to determine the amount of fuel injected:

$$\dot{m}_{fuel} = C_d A \sqrt{\frac{2 \cdot (p_{fuel} - p_{cyl})}{\rho_{fuel}}} \quad \text{(Equation 5.1)}$$

where

- C_d is the discharge coefficient of the injector nozzle
- p_{fuel} is the fuel injection line pressure in Pascals
- p_{cyl} is the in-cylinder pressure in Pascals
- ρ_{fuel} is the fuel density in kilograms per cubic metre
- A is the injector nozzle cross sectional area in square metres

The discharge coefficient is traditionally assumed to be a constant 0.7, however by determining the coefficient in relation to needle lift a more accurate calculation can be performed. Knowing the amount of fuel injected per engine cycle allows more accurate determination of how effective the fuel energy is being used.

5.3.6 Encoderless operation

It is not always possible to fit the necessary hardware to an engine to record crank angle position. For these situations only pressure data and the TDC marker need be recorded at a fixed acquisition rate, as shown in figure 5.3. Calculating the elapsed time of each engine cycle, each cycle can be divided into even crank angle degrees.

Although this method is clearly not as accurate as an engine fitted with a crank angle encoder it may have uses in areas of research or development where high accuracy is not required.

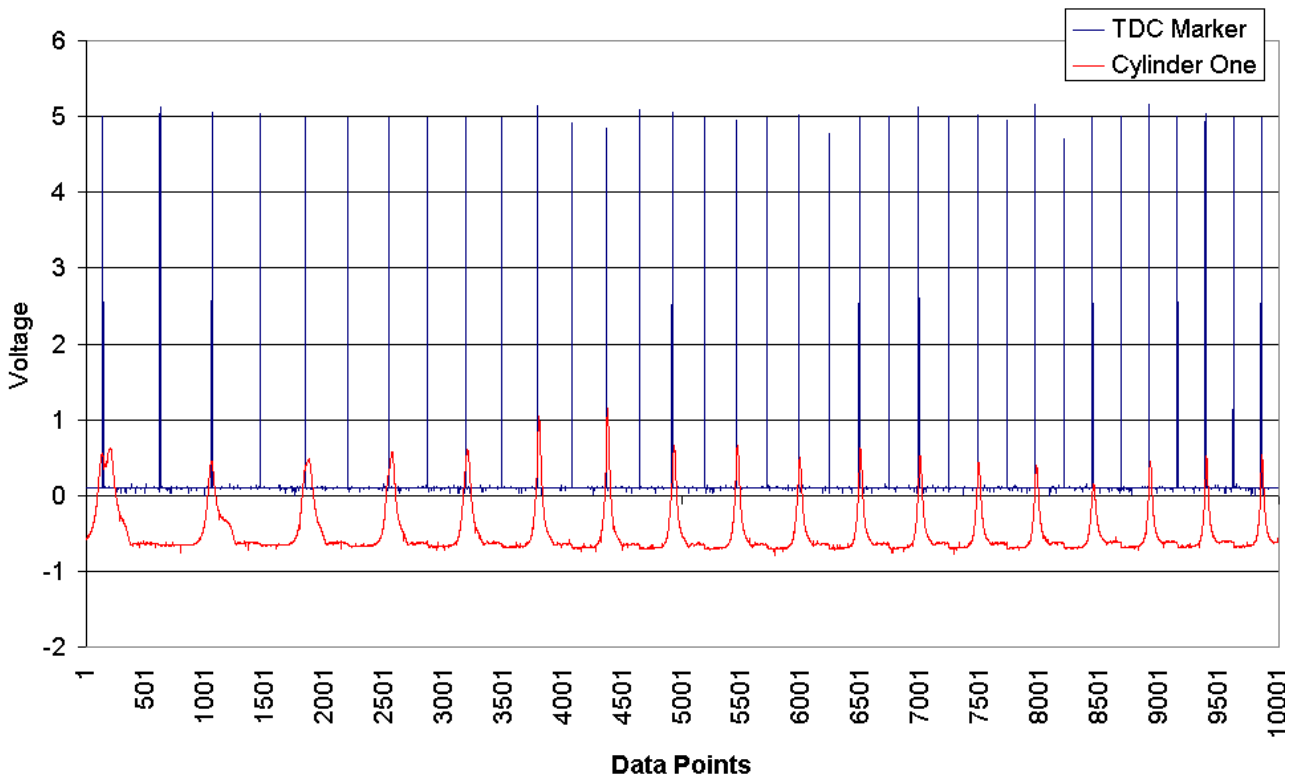


Figure 5.3 – Recorded in-cylinder pressure and TDC marker data (Rover V8 – Engine Start up)

6.0 Conclusions

This report has presented the initial work on building a combustion analysis system. The project was started by making a thorough review of current acquisition and analysis technology. This has highlighted the importance of good quality data being collected if meaningful analysis is to be carried out. In particular, errors in locating TDC introduce a large error in calculated parameters such as IMEP.

Hardware and software has been developed to put this theory into practice, and validation has been carried out to compare results with other researchers.

Additionally, several pieces of unique work were carried out:

- Calibration of dynamometer outputs
- Development of a cylinder volume equation allowing for wrist pin offset
- Handling of acquisition at incorrect TDC
- Handling of cylinder angular offset
- Determination of thermodynamic loss angle

To allow for the continuation of the project in the future, suggestions have been made for follow on work and improvements.

The original aim of the project, as outlined in the preparation report, was to “provide a documented system of internal combustion engine cylinder pressure data acquisition and analysis.” This aim has been achieved by the software outlined in this report and is documented by this report and the user guide contained within the appendix.

7.0 References

1. Brunt, M. F. J., Pond, C. R., "Evaluation of Techniques for Absolute Cylinder Pressure Correction," SAE Paper 970036, 1997
2. Brunt, M. F. J., Emtage, A. L., "Evaluation of Burn Rate Routines and Analysis Errors," SAE Paper 970037, 1997.
3. Brunt, M. F. J., Pond, C. R., Biundo, J., "Gasoline Engine Knock Analysis using Cylinder Pressure Data", SAE Paper 980896, 1998.
4. Rai, H. S., Brunt, M. F. J., Loader, C. P., "Quantification and Reduction of IMEP Errors Resulting from Pressure Transducer Thermal Shock in an S.I. Engine," SAE Paper 1999-01-1329, 1999.
5. Checkel, M. D., Dale, J.D., "Computerized Knock Detection from Engine Pressure Records," SAE Paper 860028, 1986.
6. Brunt, M. F. J., Rai, H., Emtage, A. L., "The Calculation of Heat Release Energy from Engine Cylinder Pressure Data," SAE Paper 981052, 1998.
7. Ganesan, V., "Computer Simulation of Spark-ignition Engine Processes," University Press (India) Limited, Hyderabad, India, 1996.
8. Stone, R., "Introduction to Internal Combustion Engines," Macmillan Press Limited, Basingstoke, Hampshire, 1999.
9. Morishita, M., Kushiya, T., "An Improved Method of Determining the TDC Position in a PV-Diagram (First Report)," SAE Paper 970062, 1997.
10. Randolph, A. L., "Methods of Processing Cylinder-Pressure Transducer Signals to Maximize Data Accuracy," SAE Paper 900170, 1990.
11. Lancaster, D. R., Krieger, R. B., Lienesch, J. H., "Measurement and Analysis of Engine Pressure Data," SAE Paper 750026, 1975.
12. Kim, K. S., Kim, S. S., "Measurement of Dynamic TDC in SI Engines Using Microwave Sensor, Proximity Probe and Pressure Transducers," SAE Paper 891823, 1989.
13. Rassweiler, G. M., Withrow, L., "Motion Pictures of Engine Flames Correlated with Pressure Cards," SAE Proceedings May 1938, 1938.
14. Brunt, M. F. J., Emtage, A. L., "Evaluation of IMEP Routines and Analysis Errors," SAE Paper 960609, 1996.
15. Cheung, H. M., Heywood, J. B., "Evaluation of a One-Zone Burn-Rate Analysis Procedure Using Production SI Engine Pressure Data," SAE Paper 932749, 1993.

16. Brunt, M. F. J., "The Effect of Combustion Chamber Design on The Combustion Rate in An SI Engine," PhD Thesis, Loughborough University of Technology, 1980.
17. Hayes, T. K., Savage, L.D., "Cylinder Pressure Data Acquisition and Heat Release Analysis on a Personal Computer," SAE Paper 860029, 1986.
18. Rocco, V., "D.I. Diesel Engine In-Cylinder Pressure Data Analysis Under T.D.C. Setting Error," SAE Paper 930595, 1993.
19. Amann, C. A., "Cylinder-Pressure Measurement and Its Use In Engine Research," SAE Paper 852067, 1985.
20. Brunt, M.F.J., Lucas, G. G., "The Effect of Crank Angle Resolution on Cylinder Pressure Analysis," SAE Paper 910041, 1991.
21. Heywood, John, "Internal Combustion Engine Fundamentals," McGraw-Hill Book Company, New York, 1988.
22. Lucas, G. G., "Engines," Departmental Publication No. 27, AAE Department, Loughborough University, 1997.
23. Hohenberg, G., "Advanced Approaches for Heat Transfer Calculations," SAE Paper 790825, 1979.
24. Annand, W. J. D., "Heat Transfer In The Cylinders Of Reciprocating Internal Combustion Engines," Proc. I. Mech. E., Vol. 177, No. 36, pp. 973-989, 1963.
25. Woschni, G., "A Universally Applicable Equation for the Instantaneous Heat Transfer Coefficient in the Internal Combustion Engine," SAE Paper 670931, 1967.
26. Street, R., Watters, G., Vennard, J., "Elementary Fluid Mechanics: Seventh Edition," John Wiley & Sons, Inc., New York, USA, 1996.
27. Robert Bosch GmbH, "Automotive Handbook: Second Edition," Stuttgart, Germany, 1986.
28. Wray, A. P., Ibrahim, S. S., Carrotte, J. F., "Engineering Thermodynamics," Departmental Publication No. 18, AAE Department, Loughborough University, 1997.
29. Burton Performance Centre Limited, "2000 Burton Power Catalogue," Burton Performance Centre Limited, Ilford, 2000.
30. Leifert, Dr. T., "TDC-Sensor AVL 428," AVL List GmbH, Graz, Austria, 1998.
31. Tazerout, M., Le Corre, O., Rousseau, S., "TDC Determination in IC Engines Based on the Thermodynamic Analysis of the Temperature-Entropy Diagram," SAE Paper 1999-01-1489, 1999.
32. Douglas, R., Kee, R. J., Carberry, B. P., "Analysis of In-Cylinder Pressure Data in Two-Stroke Engines," SAE Paper 972792, 1997.

33. Young, M. B., Lienesch, J. H., "An Engine Diagnostic Package (EDPAC) – Software for Analyzing Cylinder Pressure-Time Data," SAE Paper 780967, 1978.
34. Randolph, A. L., "Cylinder-Pressure-Based Combustion Analysis in Race Engines," SAE Paper 942487, 1994.
35. Schmidt, F. W., Henderson, R. E., Wolgemuth, C. H., "Introduction to thermal sciences," John Wiley and Sons, New York, 1993.
36. Holman, J. P., "Heat Transfer, 8th edition," McGraw-Hill, Inc., New York, 1997.
37. Incropera, F. P., de Witt, D. P., "Introduction to Heat Transfer: Second Edition," John Wiley and Sons, New York, 1990.
38. Brown, B. R., "Determination of Knock Screening Metrics and Calibration of Centre Frequencies," Internal Report PSD-2000-145, Ford Motor Company, 2000.

Appendix A: Technical Specifications

Rover V8

- 3947cc, V8
- Bore 94mm
- Stroke 71.1mm
- Compression Ratio 9.4:1
- Firing Order 1,8,4,3,6,5,7,2
- Connecting rod length assumed 160mm
- Pin offset assumed zero
- Max Power 115 kW @ 5000RPM
- Max Torque 280 Nm @ 2750RPM

National Instruments 6024E Multifunction I/O Card

- PCI Interface
- 8 Differential Channels
- 12-bit Resolution
- 200kHz maximum sampling rate (one channel)
- Digital Trigger
- External Clock

National Instruments BNC-2090 Shielded BNC Adapter Chassis

- Provides BNC connectors for inputs, outputs, trigger and external clock

Kistler 6121/6125A piezoelectric pressure transducer

- 0 – 250 bar range
- Natural frequency of 75kHz (6125A) and 100kHz (6121)
- -50 to 350°C temperature range

Kistler 5011 charge amplifier

- Configurable ranges and time constants
- Choice of analogue lowpass filters

Viglen Genie P3 550

- Intel Pentium 550 MHz CPU
- 128Mb RAM
- 12Gb Hard Drive
- Windows 95 Operating System
- 120Mb Superdrive

Appendix B: Equipment Calibration

Kalibrierblatt
Feuille d'étalonnage
Calibration sheet

Piezo-Instrumentation

KISTLER

Drucksensor
Capteur de pression
Pressure Sensor

Type 6125A SN 573780

Kalibrierter Bereich Gamme étalonnée Calibrated range	[bar]	0...250	0...50	Betriebstemperaturbereich Gamme de temp. d'utilisation [°C] -50...350 Operating temperature range
Empfindlichkeit Sensibilité Sensitivity	[pC/bar]	-15,8	-15,9	Kalibriert bei Étalonné à [°C] 20 Calibrated at by Sh Date 11.11.95
Linearität Linéarité Linearity	≤±%FSO	0,1	0,1	1 bar = 10 ⁵ N · m ⁻² = 1,019... at = 14,50... psi 1 at = 1 kp · cm ⁻² = 1 kgf · cm ⁻² = 0,980665 bar 1 psi = 0,06894... bar
* Empfindlichkeitswert bei * Sensibilité à * Sensitivity at	200 °C 350 °C	-15,8 -15,7	-15,9 -15,7	* Hochtemperatur-Kalibrierung * Étalonnage à température élevée * High Temperature Calibration

Kalibrierung rückführbar auf das Eidgenössische Amt für Messwesen
Étalonnage imputable à l'Office fédéral de métrologie
Calibration traceable to the Swiss Federal Office of Metrology

Terminologie nach ANSI/ISA-S37.1-1975 (R1982)
Terminologie d'après ANSI/ISA-S37.1-1975 (R1982)
Terminology per ANSI/ISA-S37.1-1975 (R1982)

Linearität: Beste Gerade durch den Nullpunkt
Linéarité: Meilleure droite par le zéro
Linearity: Best straight line through zero

Dr 683 6053A Ed. 3.94

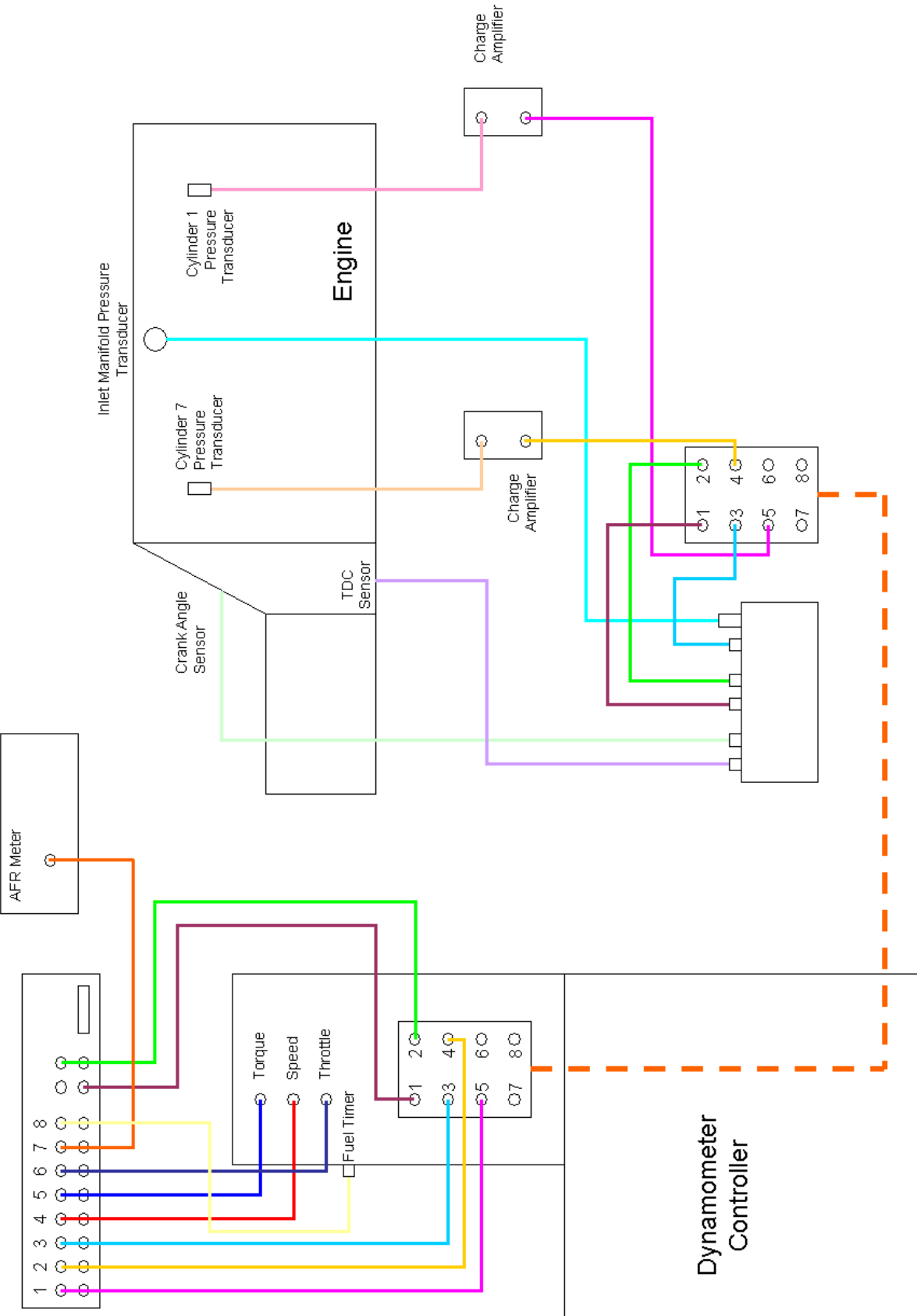
Kistler Instrumente AG Winterthur, CH-8408 Winterthur, Schweiz

Tel. (052) 224 11 11, Fax (052) 224 14 14

Figure B.1 – Kistler 6125A calibration sheet (SN 573780)

Appendix C: User Guides

C.1 Hardware Setup



C.2 Realtime Acquisition

Before commencing data acquisition the engine should be inspected for any obvious sign of problems such as leaking water or parts missing from the engine. Turn on the charge amplifiers and press the Operate button. The charge amplifiers calibration should be stored when the units are switched off so this will not need setting. All coax connections should be broken and reconnected, both around the engine and on the dynamometer controller. The engine can then be started and allowed to warm up.

The realtime acquisition software is called `Realtime Display.vi` and can be loaded by double-clicking on its icon. The main panel is shown in figure C.1. Ambient air temperature and pressure should be determined and entered into the main panel. This will determine air density for the volumetric efficiency calculation.

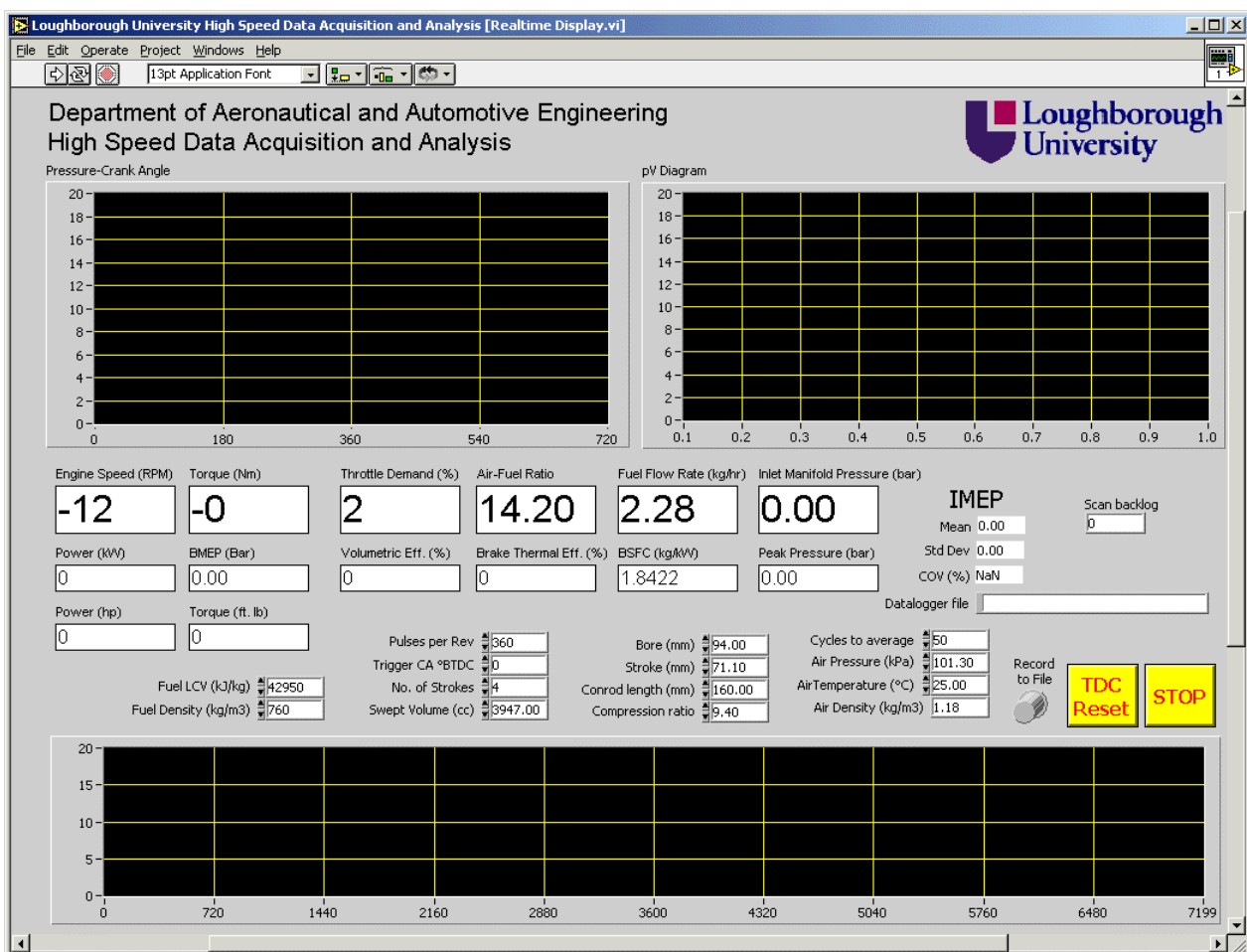


Figure C.1 – High speed data acquisition and analysis main panel

Data acquisition started by clicking the  button. If the acquisition is triggered by exhaust TDC, rather than induction TDC, the **TDC Reset** button can be used to restart acquisition. Peak pressure should now be occurring around the 360-degree mark.

To log acquired and calculated parameters ensure the filename is specified on the panel as **Datalogger file** and press the **Record to File** button. Data is appended to any existing logger results and is in a format that can be loaded by Microsoft Excel.

C.3 Data Analysis

Analysis of engine performance consists of four steps:

- Recording data to disk
- Converting data to binary format
- Running analysis
- Loading results into Excel

Recording data to disk

The user should start the engine on the dynamometer and allow the engine to reach operating temperature before recording any data. As with realtime analysis the charge amplifiers should be switched on and all coax connections broken and then reconnected.

Load the *Acquire Cylinder Data.vi* by double-clicking on its icon. The main panel should be loaded as shown in figure C.2.

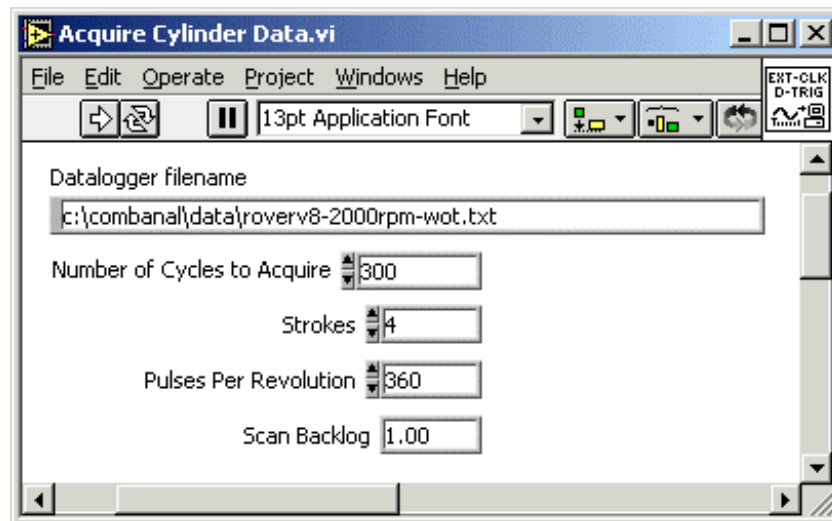


Figure C.2 – Acquire Cylinder Data.vi main panel

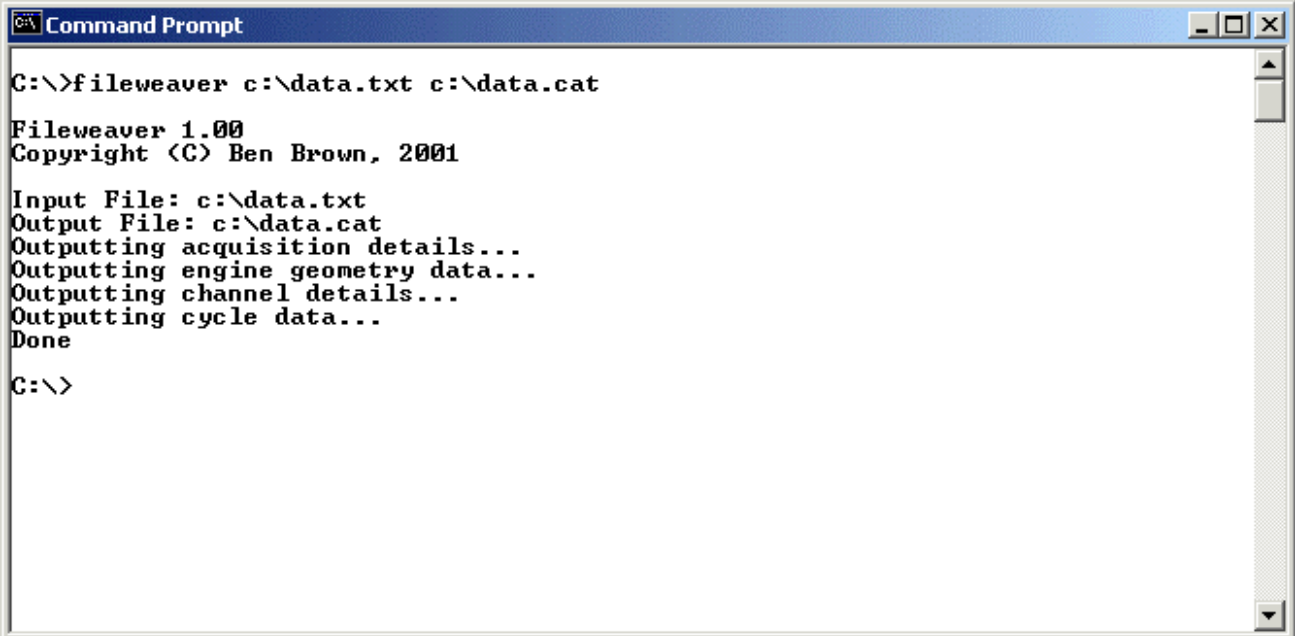
Set the **datalogger filename** and number of cycles to acquire to suit. The number of strokes and pulses per revolution should already be set for the engine in use. Once you are ready to start data acquisition press the  button. If the filename already exists you will be prompted to replace the file or cancel the acquisition. The start button will change to , indicating acquisition is in progress. Once the acquisition is complete either quit the panel using the  icon in the top right hand corner of the window or repeat the process to continue acquiring data.

Converting data to binary format

The following two steps require you to have an open command prompt, as shown in figure C.2. This can be loaded from the  menu in Windows.

The *fileweaver* program can then be used to convert the acquired data to binary file format. This is required to reduce the size of the data and allow importation of the data into the combustion analysis software.

The example shown in figure C.3 uses the acquired data located at `c:\data.txt` and the resulting binary file is saved as `c:\data.cat`.



```
C:\>fileweaver c:\data.txt c:\data.cat

Fileweaver 1.00
Copyright (C) Ben Brown, 2001

Input File: c:\data.txt
Output File: c:\data.cat
Outputting acquisition details...
Outputting engine geometry data...
Outputting channel details...
Outputting cycle data...
Done

C:\>
```

Figure C.3 – Running binary file conversion (fileweaver)

Running analysis

From the command prompt window the CAT (Combustion Analysis Tool) can be run. In the following example, figure C.4, the input file is the `c:\data.cat` file created previously and the output file is `c:\output.txt`.

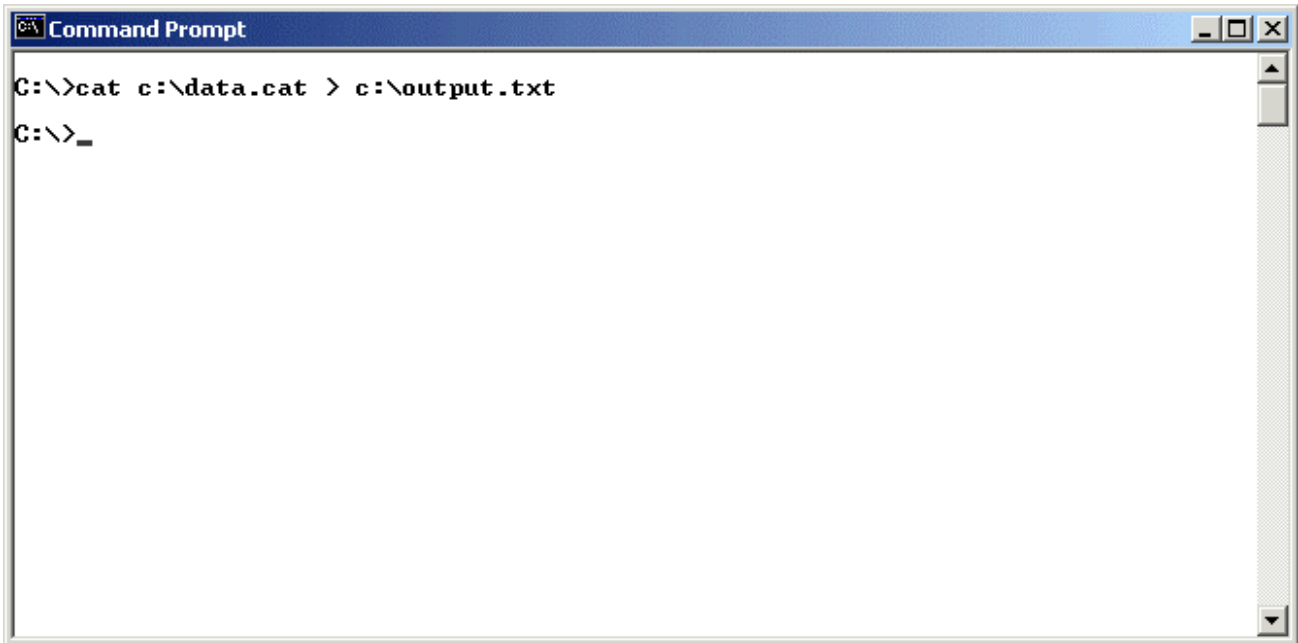


Figure C.4 – Running combustion analysis (CAT)

Loading results into Excel

Use the File - Open menu in Excel to load a new file. Select the file type as any and select the output file, in this case `c:\output.txt`.

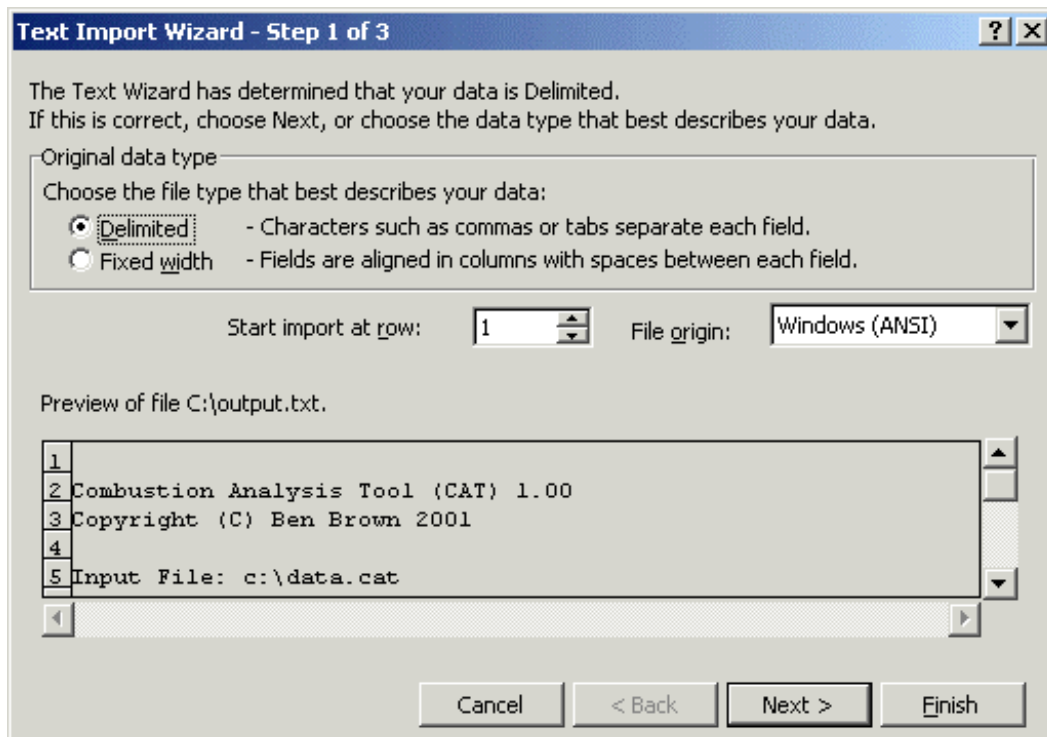


Figure C.5 – Excel text import wizard, step one

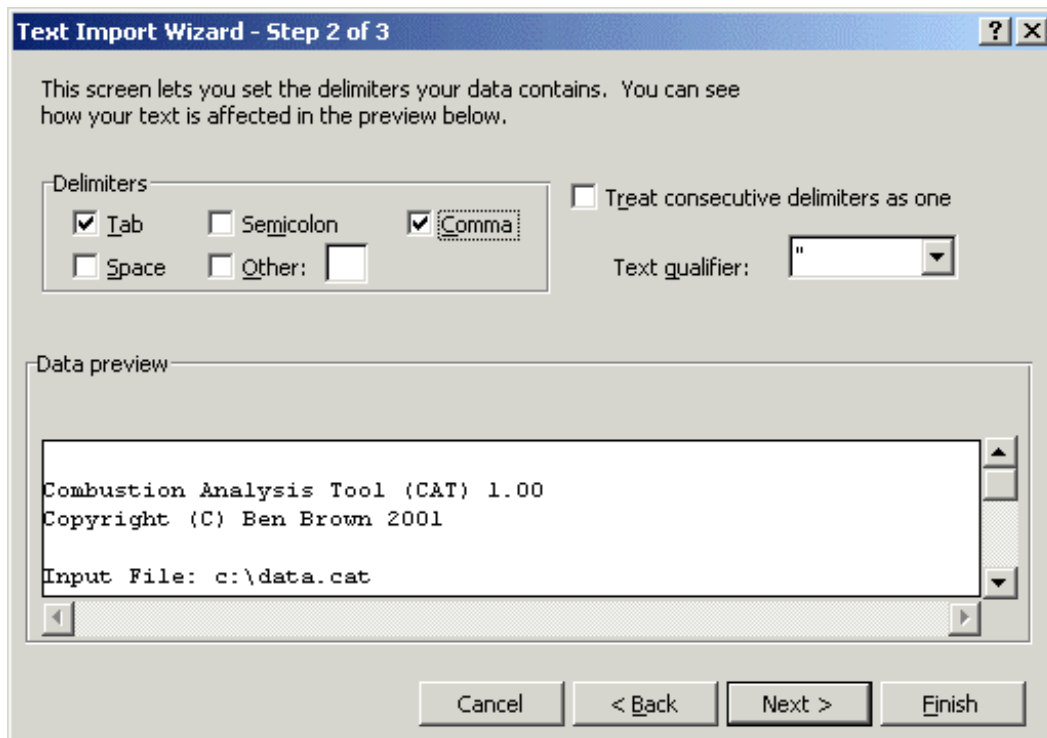


Figure C.6 – Excel text import wizard, step two

In the text import wizard select Delimited file type and click Next in the first window, select the comma icon in the second and then click Finish.

The file will now be loaded into Excel. The file consists of two sections. The first is data calculated on a crank angle basis for the first engine cycle. The data is arranged in headed columns. The second section is the cycle-by-cycle parameters for each cycle, such as location of peak pressure. The graphing capabilities of Excel can then be used to graph the data one is interested in.

Appendix D: CD-ROM Contents

A CD-ROM is attached containing programs, data and research gathered during the course of the project. This is split into a number of directories as outlined below:

Programs\Realtime Display

The LabVIEW files required for the real time acquisition and analysis.

Programs\High Speed Engine Data Acquisition

The LabVIEW file for saving data to disk for later analysis.

Programs\CAT

The combustion analysis software, CAT (Combustion Analysis Tool), and the fileweaver software for converting acquired data into binary file format.

Programs\File Formats

lfile-e.doc	AVL I-File format specification
DSP.doc	DSP file format specification
CAT File Format.txt	The binary file format used by CAT

Data

Data acquired from the Rover V8 engine in spreadsheet file format. Filename indicates engine speed and load.

Research

Brouchures and catalogues for software and hardware used in combustion analysis.

Manuals

Manuals for the National Instruments data acquisition hardware.

Appendix E: Timing Plan

Appendix F: Project Costs

The project utilised hardware that had already been purchased by the department. However, if the equivalent hardware were to be purchased the costs are outlined below.

PC (Viglen PIII-1000, 128Mb RAM, 30Gb HD)	£850
National Instruments PCI-6024E acquisition card	£595
National Instruments BNC-2090 BNC adaptor chassis	£325
Kistler 5011 Charge Amplifier (including case)	£1680
Kistler 6125A Transducer	£1492
Total	£4942

Acquiring additional cylinder data would require one extra transducer and one extra charge amplifier, i.e. an extra £3172. The acquisition card is capable of acquiring eight channels of data and is available without analogue output, the PCI-6023E, for £395.

A spark plug transducer such as the Kistler 6117 costs £1858.